

Accepted Manuscript

Quantitative material releases from products and articles containing manufactured nanomaterials: Towards a release library

Antti Joonas Koivisto, Alexander Christian Østerskov Jensen, Kirsten Inga Kling, Asger Nørgaard, Anna Brinch, Frans Christensen, Keld Alstrup Jensen



PII: S2452-0748(16)30101-X
DOI: doi: [10.1016/j.impact.2017.02.001](https://doi.org/10.1016/j.impact.2017.02.001)
Reference: IMPACT 56

To appear in: *NANOIMPACT*

Received date: 2 September 2016

Revised date: 3 February 2017

Accepted date: 7 February 2017

Please cite this article as: Antti Joonas Koivisto, Alexander Christian Østerskov Jensen, Kirsten Inga Kling, Asger Nørgaard, Anna Brinch, Frans Christensen, Keld Alstrup Jensen, Quantitative material releases from products and articles containing manufactured nanomaterials: Towards a release library. The address for the corresponding author was captured as affiliation for all authors. Please check if appropriate. Impact(2017), doi: [10.1016/j.impact.2017.02.001](https://doi.org/10.1016/j.impact.2017.02.001)

This is a PDF file of an unedited manuscript that has been accepted for publication. As a service to our customers we are providing this early version of the manuscript. The manuscript will undergo copyediting, typesetting, and review of the resulting proof before it is published in its final form. Please note that during the production process errors may be discovered which could affect the content, and all legal disclaimers that apply to the journal pertain.

Quantitative material releases from products and articles containing manufactured nanomaterials: Towards a release library

Antti Joonas Koivisto,^{*,a} Alexander Christian Østerskov Jensen,^a Kirsten Inga Kling,^a Asger Nørgaard,^a Anna Brinch,^b Frans Christensen,^b Keld Alstrup Jensen^a

^aNational Research Centre for the Working Environment, Lersø Parkallé 105, Copenhagen DK-2100, Denmark.

^bCOWI A/S, Parallelsvej 2, Kongens Lyngby DK-2800, Denmark.

*Corresponding author phone: +45 3916 5200, e-mail: jok@nrcwe.dk

Abstract

Environmental and human risk assessment models are critical for estimating the impact of nanomaterials on the ecosystem and human health. Realistic exposure estimates usually require quantitative process-specific release and emission characteristics in specific exposure situation. For nanomaterial-based products, release data suitable for modelling are currently very scarce. Consequently, in this study, we reviewed the release assessment literature and extracted or derived quantitative releases, as well as properties of released fragments from 374 different scenarios on nanomaterial-based products and articles, including artificial weathering, mechanical treatment, spraying, washing and leaching. The release literature has assessed textiles, thermosets, thermoplastics, coated surfaces, sprays, incineration, and other articles and the results are provided for different release processes. Artificial weathering of composites at a UV-dose of *ca.* 150 MJ m⁻² released 10¹ to 10⁵ mg·m⁻² fragments containing nanomaterials and *ca.* 10⁻⁴ to

$10^3 \text{ mg}\cdot\text{m}^{-2}$ nanomaterials. Mechanical treatment released from *ca.* 9×10^4 to 3.1×10^{10} particles $\cdot\text{s}^{-1}$.

Components treated mechanically after artificial weathering released up to *ca.* 2.7×10^6 particles $\cdot\text{s}^{-1}$. Pump sprays and propellant sprays on average emitted 1.1×10^8 and 8.6×10^9 particles $\cdot\text{g}^{-1}$, respectively. First wash and rinse of textiles containing Ag NM released 0.5 to 35 % of the initial elemental Ag-concentration while textiles containing TiO_2 NM released 0.01 to 3.4 % of the initial elemental Ti-concentration. Incineration produced mainly soot at yield ranging from 1 to 39 wt.% where NM additives may be present depending on the incineration conditions. The characteristics of the released particles varied from consisting of pure NM to fully matrix-embedded NM depending on the products and processes. The results from this study form the basis for a quantitative release library for products containing nanomaterials. We concluded that the release assessment field should harmonize the test procedures and data reporting, including quantification of the amount of nanomaterials released when possible. This would improve the applicability of the data to measure and model human and environmental exposure to nanomaterials and the associated risks.

Keywords

Nanomaterial, Release, Emission rate, Environmental exposure, Personal exposure.

Abbreviations

ABS poly(Acrylonitrile Butadiene Styrene)

AC Acrylate coating

APS Aerosol particle sizer

CB Carbon Black

CNF	Carbon nanofiber
XPU	Cross-linked polyurethane
CNT	Single and multi-walled Carbon Nanotube
CPC	Condensation particle counter
CSH	Calcium silicate hydrates
DGEBA	Diglycidyl ether of bisphenol A
EC	Elemental Carbon
ELPI	Electrical low pressure impactor
EVA	Ethyl vinyl acetate
FB	Fireboard
FMPS	Fast mobility particle sizer
GO	Graphene oxide
HNT	Halloysite nanotube
MAT	Matrix
MMT	Montmorillonite
MRR	Material removal rate
N/A	Not analysed
NIST	The National Institute of Standards and Technology

NM	Nanomaterial
NR	Natural rubber
OC	Organic carbon
OPC	Optical particle counter
PA6	Polyamide 6
PBT	Polybutylene terephthalate
PC	Polycarbonate
PES	Polyester
PET	Polyethylene terephthalate
PMMA	Polymethyl methacrylate
POM	Polyoxymethylene
PP	Polypropylene
PS	Polystyrene
PU	Polyurethanes
PVC	Polyvinyl chloride
REACH	Registration, Evaluation, Authorization, and Restriction of Chemicals
SGA	Manual gravity spray gun
SMC	SprayMax®-can

SMPS	Scanning mobility particle sizer
SPHERE	Simulated Photodegradation via High Energy Radiant Exposure
SSC	Standard spray can
TA	Taber Abraser
TEM	Transmission electron microscopy
TPU	Thermoplastic polyurethane
VOC	Volatile organic compounds

1. Introduction

Nanotechnology involves the ability to design materials from the atomic to *ca.* 100 nm scale and produce novel materials and products with superior properties and functionalities. The increasing number of marketed products based on nanotechnology (here referred to as NM-products; Vance *et al.*, 2015) has raised concerns regarding their potential environmental implications and risks (Juganson *et al.*, 2015; Tolaymat *et al.*, 2015; Massatsky *et al.*, 2014; Dwivedi *et al.*, 2015; Mitrano *et al.*, 2015a). Besides potential release during application, NM-products may be subject to physical and chemical stress such as mechanical abrasion, UV irradiation, and leaching (rain, wash) during their life cycle, which may lead to release of material with new nano-enabled properties or full release of added NMs.

The form of the released NM depends on material physical and chemical properties, release mechanism, and the environmental conditions during release as well as the level of material-aging (Dwivedi *et al.*, 2015; Mitrano *et al.*, 2015a; 2015b). Previous studies have shown that matrix containing NMs are mainly released

embedded in, associated with the matrix, or ionic form (see review studies Nowack *et al.*, 2012; 2013; Schlagenhauf *et al.*, 2014; Shandilya *et al.*, 2014; Kingston *et al.*, 2014; Froggett *et al.*, 2014; Duncan and Pillai, 2015; Duncan, 2015; Mackevica and Hansen 2016). Once fragments from NM-products are released, their fate and possible subsequent NM release and transformation depends on the surrounding conditions. In this regard, it is important to note that most toxicological studies are conducted on pure NM (Srivastava *et al.*, 2015). Several studies have found that NMs may interact differently with the biological and ecological system as compared to their non-NM counterparts while the toxicity of fragments from NM-products is matrix-dependent, regardless of a possible NM content. For example, intratracheal instillation studies have shown that inflammatory and genotoxic effects of POM and concrete sanding dusts were not increased when CNTs were added to the matrix (Wohlleben *et al.*, 2011) and sanding dust from NM paints on wooden-plates did not generate increased pulmonary inflammation or oxidative stress as opposed to pristine NMs (Saber *et al.*, 2012a; 2012b). In an oropharyngeal aspiration study, the toxicity of UV irradiated paint dusts with Ag, TiO₂, and SiO₂ NMs was found to be reduced as compared to the toxicities of the pristine NMs (Smulders *et al.*, 2014). Furthermore, exposing *Drosophila* to fragments of environmentally aged epoxy containing CNT did not reduce survivorship, while pristine CNTs reduced survivorship at all doses (Ging *et al.*, 2014). These studies indicate that pristine NM cannot be used to estimate toxicities of released fragments containing NM in environmental exposure scenarios. Thus, it is suggested that (eco-)toxicological studies of NMs should also be made using material released during intended use and simulated NM-product release scenarios (Grassian *et al.*, 2016).

Considering the impact of environmental and personal exposure to NM-products, the physico-chemical properties of the released materials drive the mechanisms of toxicity, while the fraction released defines the exposure (Harper *et al.*, 2015). The mechanisms of material release from products and articles can be divided in to several categories: passive diffusion, dissolution, and desorption of the added NMs into liquid media (Duncan and Pillai, 2015); and matrix degradation including photo-degradation, thermal decomposition, mechanical treatment, and hydrolysis (Duncan, 2015). Previous NM release review studies

(Nowack *et al.*, 2012; 2013; Schlagenhauf *et al.*, 2014; Shandilya *et al.*, 2014; Kingston *et al.*, 2014; Froggett *et al.*, 2014; Duncan and Pillai, 2015; Duncan, 2015; Mackevica and Hansen 2016) address the importance of thoroughly estimating the NM release potentials in order to correctly evaluate the potential human exposure and associated health risks. However, those studies provide usually concentrations in specific experimental setup which cannot be used as such to estimate environmental or personal exposure levels. Therefore, the release studies should report quantitative releases (*e.g.* $\text{mg}\cdot\text{mL}^{-1}$, $\text{mg}\cdot\text{kg}^{-1}\cdot\text{wash}^{-1}$, $\text{mg}\cdot\text{m}^{-2}\cdot\text{year}^{-1}$, $\text{mg}\cdot\text{s}^{-1}$) which are vital for exposure assessment as well as comparison of results from different studies.

In this review, we defined quantitative release and calculated them using the information provided by the release assessment literature for products and articles containing NMs and the forms of released fragments respectively. The goal was to advance the development of a library that contains the release data from nano-enabled products. Such a suite of release data in harmonized format is essential for improving modeling-based assessments of occupational and consumer exposure as well as the flow of NMs into the environment along the material and product life-cycle (Caballero-Guzman *et al.*, 2016). Finally, we point out current research needs and knowledge gaps in the characterization of NM release. Establishment of such a library on with high-quality release data and characteristics of the particle release is highly warranted by modelers of human and environmental risks.

2. Literature review

A total of 96 peer-reviewed scientific publications were identified as relevant original papers considering release of NMs from consumer products and articles where quantitative releases were extracted from 36 studies. Cosmetics, medical applications, and food products were excluded because of more stringent safety regulations and self-evident dosing (*e.g.* the NM dose from food products is 100%). The studies were

divided into six article groups following the outline suggested by Frogget *et al.* (2014): 1.) Thermosets; 2.) Thermoplastics; 3.) Coated surfaces; 4.) Sprays; 5.) Textiles; 6.) Other articles.

We defined quantitative release as the amount of mass released from a nanoapplication under experimental setups (scenarios) that intend to simulate situations that result in the liberation of material. Quantitative release was calculated from the measured average concentration levels and volumes of immersion fluid or dilution air, when the process and material characteristics were known as:

$$R_p = V_d * (C_f - C_i) / NF, \quad (1)$$

Where R_p is the release by process p , V_d is the dilution volume, C_f is the mean concentration during the process or final concentration in e.g. in leachates, C_i is the concentration before process or initial concentration of the leachate, and NF is the normalization factor such as process time (min), wash and rinse cycle (-), amount of product used in mass (g) or volume (mL), or applied energy (MJ). This provides a first order approximation of the quantitative releases assuming full mixing in the measured volume and insignificant sampling losses.

We were able to estimate quantitative releases for the following seven release categories: 1) Artificial weathering, 2) Mechanical treatment, 3) Mechanical treatment of artificially weathered articles, 4) Washing and leaching of textiles, 5) Use of spray products, 6) Incineration, and 7) Other articles. The results are summarized in Figures 1-5 and properties of released fragments are shown in summary tables at Supporting Information (Tables S1-S6). Data to estimate the quantitative releases was missing in 60 of the reviewed studies. However, we extracted information about the experimental techniques, and properties of the released fragments categorized as by Frogget *et al.* (2014) are in Tables S1-S6.

Recently, free NM was defined as NM which is not associated with matrix material (Wohlleben *et al.*, 2014; Duncan, 2015). In another study by Shandilya *et al.* (2016) they considered TiO₂ to be free if the content of

TiO₂ in the fragment was over 90 wt.%. Here we assume that released free NM properties are closely comparable or equal to pristine NM properties.

2.1 Release from artificial weathering

Outdoors, articles are exposed to UV irradiation and chemical (*e.g.* rain) and mechanical stress (*e.g.* wind). In artificial weathering experiments this stress is mimicked using accelerated weathering systems by exposing articles to UV irradiation and optionally to artificial rain and/or wind. The polymer degradation under accelerated laboratory weathering conditions has been shown to mimic the main outdoor weathering behavior well (Lv *et al.*, 2015). The UV dose used in the laboratory can be linked to the equivalent outdoor UV dose. For example, the estimated UV dose for the wavelengths between 295 and 385 nm at 24° to 31° N latitude (*e.g.* Florida) is *ca.* 285 MJ·m⁻² per year (Robinson *et al.*, 2011). Unless otherwise stated in the studies, UV dose [MJ·m⁻²] was calculated multiplying irradiation [W m⁻²] with irradiation time [s] and released mass was obtained from given specimen mass difference before and after exposure or (unless given by authors) calculated from leachate concentration and leachate volume. The release R due to UV irradiation was described using the following relation as formerly given by Wohlleben *et al.* (2014):

$$R = a \cdot D^b, \quad (2)$$

where R is release [mg·m⁻²], D is UV dose [MJ·m⁻²], and a [mg·MJ⁻¹] and b [-] are fitting factors. The release function is analogous to Schwarzschild's law which is used to predict irradiation photo responses (Martin *et al.*, 2003). Schwarzschild's law equals to a reciprocity law at $b = 1$, which assumes the photo response to be linearly proportional to the UV dose. The resulting fitting parameters are available in Table S8.

One third of the reviewed irradiation studies were performed using an accelerated weathering device called SPHERE (Chin *et al.*, 2004). In SPHERE, a square film of 6.25 cm² (2.5 cm × 2.5 cm) is fitted into a

holder with a circular exposure area of 2.83 cm^2 (1.9 cm in diameter). Ging *et al.* (2014) provide the exact surface area for both UV exposure and leaching. For other studies using SPHERE, we assumed that the leaching surface area is the same as the UV exposure surface area (2.83 cm^2). The release studies are rarely comparable because the exposure conditions, sampling, and analysis techniques effects on the release, except for few homogeneous datasets, such as (Wohlleben *et al.* 2016). For example, specimen mass difference before and after exposure include also moisture uptake or release from specimen as well other gas phase compounds release which is not directly comparable with *e.g.* particle release measured from run-off waters. Here, Nguyen *et al.* (2011), Petersen *et al.*, (2014) and Bernard *et al.*, (2011) used the same experimental procedure which results are comparable. Al-Kattan *et al.*, (2013) and (2015) used another experimental protocol in their studies which can be compared within as well. Rests of the studies are not directly comparable within (Table S7).

Nguyen *et al.* (2011) and Petersen *et al.* (2014) used the same test method using the same epoxy matrices (Table S1), weathering systems, and sampling techniques (Table S7). However, Nguyen *et al.* (2011) added 0.72 wt.% CNTs or 5 wt.% nano-SiO₂ to the epoxy matrix while Petersen *et al.* (2014) added 3.5 wt.% CNTs. The UV doses given by Petersen *et al.* (2014) were systematically 0.45 times lower than our calculated doses from the provided irradiation and exposure time. This may be explained by difference in the applied UV irradiation cycle used to calculate the UV dose and reported by the authors. In Petersen *et al.* (2014), the initial mass of the nanocoating was calculated from a mean dry-film thickness, surface area of the SHPERE holder (2.83 cm^2), and epoxy density of $1.1 \text{ g}\cdot\text{cm}^{-3}$. This resulted in an initial mass of $43\pm 4 \text{ mg}$, which was then used to calculate the releases (Figure 1a). The release for epoxy and epoxy containing CNTs measured by Nguyen *et al.* (2011) was *ca.* 100 and 70 times higher than the release measured by Petersen *et al.* (2014). Release function fitting parameters for epoxy were $a = 90.3 \text{ mg}\cdot\text{MJ}^{-1}$ and $b = 1.24$ for Nguyen *et al.* (2011) and $a = 4.1 \text{ mg}\cdot\text{MJ}^{-1}$ and $b = 0.96$ for Petersen *et al.* (2014) (Table S8). Nguyen *et al.* (2011) found that the mass release from plain epoxy was *ca.* 150 times higher as compared to the amount measured by Petersen *et al.* (2014) at an UV dose of $1000 \text{ MJ}\cdot\text{m}^{-2}$ (Figure 1a). When CNTs were added to

the epoxy matrix at concentrations of 0.72 wt.% (Nguyen *et al.*, 2011) and 3.5 wt.% (Petersen *et al.*, 2014), the release parameters changed to $a = 4.6 \text{ mg}\cdot\text{MJ}^{-1}$ and $b = 1.55$ and $a = 9.0 \text{ mg}\cdot\text{MJ}^{-1}$ and $b = 0.74$, respectively. Nguyen *et al.* (2011) also showed that by adding 5 wt.% of nano-SiO₂ to the epoxy, the release factor increased from 1.3 to 1.7 at UV irradiation doses from 100 to 2000 MJ·m⁻².

Sung *et al.* (2015) investigated the release of SiO₂ NM by exposing an epoxy composite containing 5 wt.% nano-SiO₂ to UV irradiation, while periodically spraying it with de-ionized water. Released elemental Si was measured from the collected run-off water and the SiO₂ release was found to be 150 mg·m⁻² at an UV dose of 1000 MJ·m⁻². This is 5600 times lower than the total mass release measured by Nguyen *et al.* (2011) Sung *et al.* (2015) used a different epoxy curing agent than Nguyen *et al.* (2011). While Sung *et al.* (2015) measured the Si concentration in run-off water, Nguyen *et al.* (2011) measured specimen mass difference before and after exposure. Sung *et al.* (2015) showed that adding nano-SiO₂ increases the total mass release, which corresponds to the results from Nguyen *et al.* (2011). At an UV dose of 1217 MJ·m⁻², the total Si release from periodically sprayed samples was *ca.* 2.2 times higher than the Si release from samples sprayed only at the end of the experiment (Figure 1b; downwards facing yellow triangle; Sung *et al.*, 2015). The release function (2) was fitted for the five highest UV doses, because there was a clear transition in release below 450 MJ·m⁻² dose (Figure 1b).

Rabb *et al.* (2010) exposed epoxy films (2.5 cm × 2.5 cm) containing 5 and 10 wt.% nano-SiO₂ NM to UV (295 – 400 nm; 480 W·m⁻²) in a SPHERE setup for 0 and 59 days corresponding to UV doses of 0 and 2450 MJ·m⁻², respectively. After simulated aging, Si was extracted by immersing the film specimens in 5 % hydrofluoric acid for 5 minutes. The release was 80 and 320 µg Si from films with 5 and 10 wt.% nano-SiO₂ exposed at 0 MJ·m⁻², and 190 and 550 µg from films with 5 and 10 wt.% SiO₂ exposed at 2450 MJ·m⁻². Nguyen *et al.* (2012) estimated later that the UV dose during the 59 day exposure was *ca.* 980 MJ·m⁻², which is 0.4 times the value calculated by Rabb *et al.* (2010).

Wohlleben *et al.* (2014) made an inter-laboratory study by weathering PA containing 3.8 wt.% nano-SiO₂ under different conditions in three different laboratories (BASF, LEITAT and NIST; Table S7). The mass release of sub-micrometer particles to immersion water was measured with *ca.* 124 (BASF) and 1100 (NIST) mg·m⁻², and the release of total mass to run-off water was 6800 mg·m⁻² (LEITAT) at an UV dose of 220 MJ·m⁻² (Figure 1a). The lowest and highest values for release were measured when the matrix was exposed to artificial rain and UV simultaneously, where degradation rates may be increased due to accelerated hydrolysis. The difference between the results obtained from the BASF and LEITAT laboratories was related to the applied sampling technique. The BASF sample was immersed in a surfactant solution under sonication for 24 hours after weathering and the sub-micrometer particle concentration was measured in the immersion solution. At LEITAT, the sample release was measured as the total mass of released particles in run-off water. In the NIST sample aged with or without artificial rain was observed *ca.* 9 times higher release than in the BASF sample even though the particle sampling protocol was the same. Deviation in the release was attributed to the different specimen temperatures during experiments (same temperature but measured either from specimen or black body radiation). In all samples, the released fragments were ranging from below 100 nm to several micrometers in diameter. Ten percent of nano-SiO₂ particles were released as single particles or agglomerates which were not bound to organics.

Wohlleben *et al.* (2011) and Hirth *et al.* (2013) carried out weathering experiments following ISO 4892-2, 2006 (Verf. A) with and without artificial rain (Table S7). Calculated UV doses were 145 and 290 MJ·m⁻², which are equivalent to 6 and 12 months of outdoor exposure at 31° N latitude, respectively. Wohlleben *et al.* (2011) estimated the CNT release from POM containing <5 wt.% CNTs to be 80 mg·m⁻² by measuring the specimens mass loss, whereas the CNT concentration was assumed to remain constant. The estimated CNT release is *ca.* 2.9 times greater than the total mass release from PU containing 3 wt.% CNT which was *ca.* 30 mg·m⁻² (Hirth *et al.*, 2013). Considering the POM CNT concentration of <5 wt.%, the CNT-release is very high compared to the total mass release from PU containing 3 wt.% CNT (Figure 1).

Hirth *et al.* (2013) showed that release from PU with 3 wt.% CNTs was *ca.* 1.3 times higher when a humidity cycle was included as compared to when it was not included (Figure 1a). The release factor $a = 8.1 \text{ mg}\cdot\text{MJ}^{-1}$ was similar to the values, (4.6 and $9.0 \text{ mg}\cdot\text{MJ}^{-1}$) estimated from measurements given by Nguyen *et al.* (2011) and Petersen *et al.*, (2014) for epoxy containing 0.72 and 3 wt.% CNTs, respectively. However, the dose exponent factor $b = 0.23$ is significantly lower for Hirth *et al.* (2013) as compared to the ones found in the two other studies (1.55 and 0.74; Table S8).

Bernard *et al.* (2011) irradiated water based PU containing 2 wt.% GO sheets using the same setup as Nguyen *et al.* (2011) and Petersen *et al.* (2014). The initial mass of the sheets was calculated by using a mean dry-film thickness, the surface area 2.83 cm^2 and a PU density of $1.0 \text{ g}\cdot\text{cm}^{-3}$ (according to the material data sheet). This results in an initial mass of $36\pm 7 \text{ mg}$ which was then used to calculate the release in $\text{mg}\cdot\text{m}^{-2}$ (Figure 1b). The results obtained from Bernard *et al.* (2011) show that the mass release was 40 times higher for PU containing 2 wt.% GO sheets as compared to PU containing 3 wt.% CNTs (Hirth *et al.*, 2013). The small exponent factor $b (<0.4)$ in both studies suggests that these releases are only weakly linked to UV dose (Table S8).

Zuin *et al.* (2014) irradiated paints containing SiO_2 , Ag and TiO_2 NMs for 500 hours with UVA (according to ISO 11507, 2007) and UVB light (Table S7). The lamp irradiation spectrum and the measured irradiation level of $0.8 \text{ W}\cdot\text{m}^{-2}$ at 313 nm yields an UVB irradiation level of *ca.* $32 \text{ W}\cdot\text{m}^{-2}$ at 250-400 nm. Including the ISO 11507, 2007 UVA irradiation, which was assumed to be *ca.* $45 \text{ W}\cdot\text{m}^{-2}$, the total UVA+UVB irradiation was *ca.* $77 \text{ W}\cdot\text{m}^{-2}$. Ag release at $149 \text{ MJ}\cdot\text{m}^{-2}$ UV dose from a paint containing 1 wt.% nano-Ag was below the detection limit of $10^{-4} \text{ mg}\cdot\text{m}^{-2}$ (Zuin *et al.*, 2014).

Zuin *et al.* (2014) used the same TiO_2 paints as Al-Kattan *et al.* (2013) and the same SiO_2 paint as Fiorentino *et al.* (2015) (Table S3). Al-Kattan *et al.* (2015) used a similar SiO_2 paint as Zuin *et al.* (2014) and Fiorentino *et al.* (2015) except that the paint contained 3 wt.% less additives and 3 wt.% more water. Fiorentino *et al.* (2015) only reported on changes in surface compositions of the nano- SiO_2 paint while Zuin *et al.* (2014) and

Al-Kattan *et al.* (2015) also reported on the NM concentrations released from the paints containing 5 wt.% SiO₂ (Figure 1b). The results showed similar release in the two studies on the SiO₂-paints. For the paints which contained 3 wt.% TiO₂, Zuin *et al.* (2014) measured 13 times higher release than Al-Kattan *et al.* (2013). This may be explained by different weathering protocols and sampling techniques. Zuin *et al.* (2014) performed sampling by leaching the weathered panels with an acetic acid solution, while Al-Kattan *et al.* (2013; 2015) measured NM particle concentrations (<450 nm) from immersion water. Further, Zuin *et al.* (2014) abraded the weathered specimens according to ISO 7784-2, 2006.

Wohlleben *et al.* (2016) weathered reference PU and PU containing, CB, SiO₂, and CNT at concentrations of 0.09 wt.% for 0, 268, and 535 MJ·m⁻² with artificial rain (Table S7). Aging at 535 MJ·m⁻² increased surface concentration of CB, SiO₂, and CNTs to 6, 5.7, and 30 %, respectively, from initial concentration of 0.09 %. Similarly as Wohlleben *et al.* (2014), they studied release of fragments from weathered surface with increasing amount of mechanical shear. Increased mechanical shear increased amount of exposed NMs. Figure 1 shows the release when the most intensive shear stress was applied (sonication) in sampling.

Wohlleben *et al.* (2016) studied evolution of primary fragments during artificial aging from NR used in car treads containing 0, 40 wt.% CB, or 40 wt.% CB and 4 wt.% CNT. The fragments were created by abrading the NR composite (Table S9) which were then exposed 0 (reference) and 720 h to UV without artificial rain in dry conditions (aging at dry road) and in continuously stirred M4 suspension (aging at surface waters). In both cases, fragments were then sampled by sonicating fragments in M4 suspension for 1 h which were analyzed and further filtered with 5 µm cutoff to and sonicated before analysis. It was found that fraction of < 1 µm particles increased substantially when sanding fragments exposed to UV were sampled using increasing shear stress. Aging in dry conditions produced 2.5 to 8.5 times more < 1 µm fragments compared to aging in M4 suspension because water absorbs efficiently UV radiation. Maximum free CNT concentration was 0.045 wt.% of the tread wear mass.

Wohlleben and Neubauer (2016) studied how the addition of NM to a matrix influences the MAT+NM release, by measuring the release after exposing the composite to single UV dose (Table S7). The releases are shown in Table S10. They concluded that quantitative release rate varies over 5 orders of magnitude by the matrix (PE, PU, PA, POM, epoxy, cement) and embedded metal-oxide, carbonaceous, or organic nanomaterials can either increase or decrease the release with less than a factor of 10. The study provides a good basis to understand the NM release from different composites, but for further understanding of the product weathering behavior, the release should be studied over a range of UV doses.

In summary, at an UV dose of *ca.* 150 MJ·m⁻², the artificial weathering resulted 10¹ to 10⁵ mg·m⁻² total mass release (MAT+NM) from the test materials and NM mass release (NM; both free and associated with matrix) from *ca.* 10⁻⁴ to 10³ mg·m⁻². On average, the release function fitting parameter *a* was 46(112) mg·MJ⁻¹ and *b* was 1.02(0.53); standard deviation in brackets. In four cases, the release was nearly directly proportional to the UV dose (*i.e.* *b* ~ 1). In one case with an epoxy material containing 5 wt.% nano-SiO₂ the material release was not continuous (Sung *et al.*, 2015). Thus, material release by weathering does not follow the reciprocity law and release should be measured as a function of UV irradiation for interpolation or should be measured directly at the UV irradiation that is appropriate for the release scenario (*e.g.* between 100 to 1000 MJ m⁻² range corresponding up to *ca.* 3.5 years of outdoor exposure).

In artificial weathering, UV-irradiation removes the polymer which results in accumulation of NM on the composite surface (Ging *et al.*, 2014; Wohlleben *et al.*, 2014; Nguyen *et al.*, 2011; 2012; Petersen *et al.*, 2014; Rabb *et al.*, 2010; Bernard *et al.*, 2011; Fiorentino *et al.*, 2015; Al-Kattan *et al.*, 2015; Wohlleben *et al.*, 2016). This is expected to provide photoprotection, as for example CNTs in XPU, PA, or POM, but may also increase the degradation rate, as for example SbZnO and in epoxy or SiO₂ in PA (Wohlleben and Neubauer, 2016). We plotted the change in release (*dR/dD*) as a function of UV dose separately for each study (Figure S1) in which were fitted a line to visualize the trend in release change (Table S8). It is expected that if NM additive reduces (increases) matrix degradation the release change should decrease (increase) as

well. However, the fitting analysis did not produce consistent results. This demonstrates that understanding the effect of NMs on the matrix degradation rate requires systematic studies on well-defined matrix materials using the same experimental, sampling and analysis techniques, and release measurements as a function of UV dose.

2.2 Release from mechanical treatment

Mechanical treatment of materials is one of the most typical release processes. Optimally, material release by mechanical treatment should be determined as the mass of material removed as function of the specific energy consumption ($\text{mg}\cdot\text{m}^3\cdot\text{MJ}^{-1}$). However, predicting the specific energy consumption is challenging because it depends on the contact properties between the tool tip and the material, which are not easily defined. In wear tests using a Taber Abrasion apparatus (Franek *et al.*, 2009), the release of airborne particles vary with the wear energy (J) (Fouvry *et al.*, 2003; Le Bihan *et al.*, 2013; Morgeneyer *et al.*, 2015) which is directly proportional to tangential force (N), *i.e.* friction force, and sliding distance (m). However, the tangential force is not measured in the standardized wear tests. Due to lack of work energy data, the releases from wear studies are only expressed as function of time. Here the quantitative releases are provided as airborne particle number emission rate (S , $\text{particles}\cdot\text{s}^{-1}$), respirable mass emission rate (S_m , $\mu\text{g}\cdot\text{s}^{-1}$), and MRR ($\mu\text{g}\cdot\text{s}^{-1}$), depending on the data available in each article. Here, if needed, the emission rates were calculated from average concentrations by assuming fully mixed concentrations, no other losses than ventilation, and process is the only source for the particles as $S = C_{\text{average}} \cdot (V_{\text{chamber}} + Q \cdot t) / NF$, where C_{average} is average concentration during the measurements t , V_{chamber} is volume of the chamber, Q is volume flow rate through the chamber, and NF is the process time t_p . This method gives a good estimate for emission rate if concentration changes are fast, *i.e.* air exchange ratio is high, and emissions are constant. If concentration time series are available, we recommend solving the particle emission rate from a convolution of the particle emission rate and particle concentration loss rate (*e.g.* Schripp *et al.*, 2008) or using time resolved

mathematical mass balance modeling (*e.g.* Koivisto *et al.*, 2012). The results are shown as Figure 2 and Table S11, the experimental protocols are available in Table S8, and the characteristics of the fragments released are available in Tables S1-S6.

Göhler *et al.* (2010) reported the total number of emitted particles during 16 second sanding of nanocoatings. Sanding was performed using a miniature sander which represents tools used in typical sanding conditions. Sanding of a two-pack PU coating containing 0 and 2.4 wt.% nano-ZnO emitted particles in number 1.8×10^7 and $2.7 \times 10^7 \text{ s}^{-1}$ (2.7×10^{11} and $4.40 \times 10^{11} \text{ m}^{-2}$), respectively.

Sachse *et al.* (2012a) showed that particle concentrations during drilling of a PA6 was reduced 20 times when 5 wt.% of MMT was added to the PA6. Sachse *et al.* (2012b) made similar experiments with reinforced PA6 containing 5 wt.% of surface modified MMT, nano-SiO₂, glass fibers and foam-glass-crystal-materials, respectively (Figure 2). Pristine PA6 was used as reference material, and yielded an emission rate of $2.8 \times 10^7 \text{ s}^{-1}$. Addition of MMT to the polymer reduced the emission rate 0.61 times, while addition of nano-SiO₂, glass fiber, and foam-glass-crystal increased the emission rates 38, 9, and 29 times, respectively.

Vorbau *et al.* (2009) measured particle concentrations during abrasion of three different coatings containing nano-ZnO. Particle concentrations were measured in a sampling hood and the collection efficiency was not defined. The MRR defined from the difference in sample weight before and after abrasion ranged from 50 to 620 $\mu\text{g}\cdot\text{s}^{-1}$.

Huang *et al.* (2012) used a lathe for sanding epoxy containing CNT in concentrations from 0 to 4 wt.%. The authors measured particle number emission rates from 2.4×10^7 to $1.2 \times 10^9 \text{ s}^{-1}$. CNT concentration did not influence significantly to the emissions but rotation speed and sand paper grit size changed the particle number emission rates. Particle number concentrations were converted to respirable mass concentrations, from which the calculated respirable mass emission rates varied from 52 to 258 $\mu\text{g}\cdot\text{s}^{-1}$.

Koponen *et al.* (2011) sanded thirteen different coatings including paints, fillers, and lacquers using a hand-held orbital sander. Sanding emissions were measured from the sanders exhaust hose, where the standard filter bag was replaced with a sampling chamber. This study was continued by Gomez *et al.* (2014) using the same orbital sander without a filter bag in a 0.66 m³ chamber. Size-resolved particle emission rates were established in cm⁻³·s⁻¹ for 3 epoxy materials and 3 paints using an aerosol dynamic model developed for the used chamber.

Schlagenhauf *et al.* (2015) abraded epoxy containing 1 wt.% CNTs labelled with radioactive Pb⁺² ions. Labelling was used to define the fraction of the protruding and free CNTs in the released fragments. The authors calculated that for each 1 g of fragments below 1 µm in diameter, the mass of protruding CNTs would be *ca.* 40 µg and free CNTs *ca.* 0.4 µg. This result can be used to estimate the potential fraction of CNTs liberated or accessible at the matrices surface. For example, a respirable mass emission rate of 258 µg·s⁻¹ (sanding epoxy containing 2 wt.% CNTs with P320 sanding paper; Huang *et al.*, 2012) corresponds to a release of up to 2 µg·s⁻¹ accessible and free CNTs.

In the case of exposure to mechanical treatment, the particle number emission rate varied 6 magnitudes from *ca.* 9×10⁴ to 3×10¹⁰ s⁻¹ (Figure 2). The emission rates from mechanical treatment are case-specific (*e.g.* Gomez *et al.* (2014) did not use tool emission controls), they strongly depend on the mixing of concentrations and experimental design. Thus, at the best, emission rates can only provide a range of emission rates for specific mechanical processes and materials. Particle number emission rates were measured using instruments with a similar particle detection range, which is essential for the comparability of the reported particle number concentration (Table S9).

2.3 Release from mechanical treatment of artificially weathered articles

The material release associated with incidental or intentional mechanical treatment of weathered articles is very relevant for NM-containing products for outdoor use. Here, is focused on mechanical treatments using different tools or artificial wind. However, mechanical shear stress is applied often also in artificial weathering studies where *e.g.* sampling procedure involves sonication (see especially Wohlleben *et al.* 2014; 2016). Here, if needed, the emission rates were calculated the same way as in mechanical treatment.

Hsu and Chein (2007) irradiated a wooden plate, a tile, and a PET film coated with a suspension containing 5 wt.% TiO₂ (thickness N/A) to UV light at 25 W·m⁻² for two hours corresponding to 2.8 hours outdoor exposure at 31° N latitude. Simultaneously, the panels were exposed to continuous artificial wind and scraped for one minute every 10 minutes using a rubber knife. The reported particle number emission rate was 4.7 s⁻¹ for measured particle concentrations of up to 633.3 cm⁻³. We consider these particle release rates as unrealistically low for the given particle concentrations.

Göhler *et al.* (2013) applied ten different pigments to acrylate and PP (Figure 3 shows materials and concentrations). Apart from TiO₂ pigment and chromium-antimony-titanium the pigments had <100 nm dimensions. Acrylate was applied to aluminum substrates. Then, coated aluminum substrates and PP composites including reference materials without pigments were exposure to UV-light and UV-light plus artificial rain, respectively (Tables S7 and S9). Weathered components were treated mechanically for 16 seconds with artificial wind, dynamic friction, or sanding. Parameters of the mechanical treatment processes were listed to ensure repeatability of the experiments. In wind erosion, the wind face velocity was 30 m·s⁻¹ which corresponds to a violent storm in the Beaufort scale (Met office, 2007). On average, the particle number emissions from artificially weathered components as compared to their new intact analogues in Al-coatings were similar during wind erosion (0.8 times lower), and 33 times higher during dynamic friction but only 4 times higher during sanding. For PP composite, on average the weathering increased 167 times in wind erosion, decreased 4.6 times in dynamic friction and decreased 2.7 times in sanding. Because the MRRs were constant between the same processes, change in release may be related

to change in the contact between the tool tip and substrate which change the size of the released fragments.

Shandilya *et al.* (2015) exposed masonry bricks coated with two different nano-TiO₂ coatings to up to 657 MJ·m⁻² UV and artificial rain. Weathered bricks were abraded using TA 5750 (Tables S7 and S9, SI). They found that abrasion of coatings can be divided into four different phases. In phase I, particle emissions increases; probably related to change of the contact surface roughness between the abrader and the nanocoating. In phase II, the abrasion process is in equilibrium and emissions are constant. In phase III, the nanocoating is partially removed from the substrate, and in phase IV, the nanocoating is fully removed and substrate particles are emitted. At a UV dose of 657 MJ·m⁻², the surface starts to crack and subsequent scratching results in removal of the surface in the form of flakes (Shandilya *et al.*, 2015). We estimated the mean particle emission rates for phases I-II (Figure 3). Only the lower limits of the particle emission rates are estimated.

For products exposed to mechanical treatment after artificial weathering, the emission rates varied over 6 orders of magnitude, from no emission detected to *ca.* $2.7 \times 10^6 \text{ s}^{-1}$ (Figure 3). This is likely because the particle number concentration is not a conservative quantity without having information about the particle size distribution and detailed physicochemical characterization to show if the released matter is released as partly evaporated. Differences in emissions between different processes may be related to change in sampling efficiency or air mixing in the experimental setup.

2.4 Release from spray processes

In a spray process, the particle emission rate (also known as overspray) is the ejection mass rate multiplied with transfer efficiency defined as the fraction of spray that coats the surface (Flynn *et al.*, 1999; Tan *et al.*, 2002a; 2002b). Transfer efficiency depends on spray applications, spray suspension properties, and the

spraying conditions and is typically in the range of 70 to 95% in industrial use (Flynn *et al.*, 1999). Airborne particle emission rates from spray processes are given as the number of particles released per second (s^{-1}) or per amount of sprayed product (g^{-1} or mL^{-1}). Here, the emission rates were calculated the same way as in mechanical treatment for Nørgaard *et al.* (2009) and Bekker *et al.* (2014) except NF was ejection mass. Losert *et al.* (2014) gives a comprehensive review of the human exposure to conventional and nanotechnology-based sprays, but they do not elaborate on the composition of the released particles and particle emission rates.

Nørgaard *et al.* (2009) used a 0.66 m^3 ($Q=16\text{ L}\cdot\text{min}^{-1}$) chamber to study VOC and particle emissions from four different nanofilm coating sprays designed for non-absorbing floor materials (pump spray), ceramic tiles (pump spray), window glass (pump spray), and a multipurpose surfaces cleaning and film coating (propellant spray). The results showed that using pump sprays resulted in airborne overspray particles ranging in size from *ca.* 10 nm to several μm at emission rates of up to $0.24\times 10^9\text{ g}^{-1}$ (Figure 4). For floor and ceramic tile products all the observed particles were considered to be generated by condensation of the active silane and siloxane compounds in the products inferred from particles found on TEM-grids exposed by direct spraying (unpublished). The glass-coating product contained nano- TiO_2 , while the multipurpose products contained several different particles, organic substances and limonene.

Quadros and Marr (2011) studied particle emissions in a 0.52 m^2 chamber from commercially available sprays, marketed to contain NMs, which were applied from pump spray dispensers. The studied sprays were an anti-odor spray, a surface disinfectant spray, and a throat spray. Use of all sprays resulted in airborne overspray particles below 100 nm. Emission rates were reported as particles released per activation (activation^{-1} and $\text{ng activation}^{-1}$) and particles released per volume sprayed product (mL^{-1}) for size classes $<0.75\text{ }\mu\text{m}$ (Figure 4) and between 0.3 to $10\text{ }\mu\text{m}$. TEM analysis of airborne particles showed that anti-odor spray particles were mainly below 100 nm in size and contained Ag and Cl.

Bekker *et al.* (2014) studied particle emissions from commercially available impregnator and antiperspirant propellant sprays that were marketed to contain NMs, and two reference propellant sprays. The experiments were performed in a 19.5 m³ experimental room without ventilation or air mixing. The measurements were performed from 30 to 100 cm and 290 to 360 cm to the spray site. The resulting average concentrations were used to calculate the emission rates (Figure 4). Airborne nano-SiO₂ particles were detected only from the antiperspirant spray, even though impregnator spray should have contained SiO₂ NM as well.

Göhler and Stintz (2014) studied particle emissions from different spray-application technologies (Figure 4). Spraying was performed using TPU coating, acrylate topcoat with TiO₂ pigment particles, water-based coating with TiO₂ pigment particles, and organic solvent-based mixed coating. ZnO, Fe₂O₃, and SiO₂ NMs were deliberately added to the spray suspensions. Particle emissions were measured in a 1235 mm long spray channel which was purged at flow rate from 200 to 300 L·min⁻¹. The influence of the setup on the transfer efficiency was not characterized, but the authors assumed that spray particles are turbulently mixed in the purge air and particle losses onto spray channel wall were negligible. This scenario was assumed to simulate spraying directly into air. Spray ejection mass flows (g s⁻¹) and particle number releases (g⁻¹) were measured for particle sizes of 0.1, 1, and 10 µm. Figure 4 shows the emission rates for particles below 10 µm in diameter. Microscopy analysis showed dried-out spray droplets containing ZnO and Fe₂O₃ NM agglomerates, TiO₂ pigment particles, and a matrix consisting of binder, hardener, filler, and dispersing agents. Isolated non-volatile particles were not detected and particles below 100 nm consisted of dried matrix droplets without non-volatile particles.

Hagendorfer *et al.* (2010) studied particle emissions from propellant spray and pump spray dispensers using a commercially available water-based spray product marketed to contain nano-Ag, and a reference product without NMs. The nano-Ag spray suspensions contained Ag agglomerates (6 nm primary particle size). Particle concentrations were measured in a 0.3 m³ chamber. Testing of the propellant gas spray dispenser

resulted in increased concentration levels of volatile sub-100 nm particles, whereas pump sprays did not increase the concentration level notably. Results from microscopy analyses of airborne particles collected with and without a thermodesorber (temperature N/A) indicated that non-volatile particles are transported in droplets rather than as free particles.

Nazarenko *et al.* (2011; 2014) studied the potential human exposure during use of eleven commercially available sprays of which, six sprays were labelled as containing NMs. They found that all spray suspensions contained particles below 10 nm (hydrodynamic size). Results from TEM analysis suggested that three spray suspensions, where presence of NM was claimed, did not contain non-volatile particles. All regular sprays contained non-volatile particles. The size of the non-volatile particles ranged from sub-100 nm in diameter to several μm , except in a skin hydrating mist, where the smallest non-volatile particles observed were 146 nm in diameter. Simulated spray application increased the airborne particle concentrations in the size range from 13 nm to over 10 μm .

Lorenz *et al.* (2011) studied particle emissions from a commercially available antiperspirant propellant spray, two different shoe impregnation propellant sprays and a plant strengthening agent pump spray dispenser. Results from TEM analysis of the spray suspensions showed that one of the shoe impregnation sprays and the plant strengthening agent contained non-volatile particles while the antiperspirant contained micron-sized structures. All propellant sprays emitted airborne particles sub-100 nm. Using the pump spray did not elevate the airborne particle concentrations from the background level. According to the TEM analysis, 86 to 91% of the airborne particles were smaller than 100 nm. NM agglomerates were found to be embedded into micrometer-sized particles.

Chen *et al.* (2010) studied particle emissions from a commercially available bathroom cleaner/sanitizer containing TiO_2 NM. The geometric mean diameter of the overspray particles was 75 nm with a 2.3 geometric standard deviation. TEM analysis of airborne particles showed TiO_2 agglomerates with diameters

ranging from 40 nm to 3.5 μm . The surfaces of TiO_2 particles were porous which according to the authors suggest that the particles were coated with suspension matrix.

Six out of nine studies found and documented free NM agglomerates with sizes from tens of nanometers to several micrometers. The overspray particle emission using pump sprays was *ca.* 1.1×10^8 (1.0×10^8) g^{-1} while the level generated using propellant sprays was *ca.* 8.6×10^9 (3.8×10^9) g^{-1} (standard deviation in brackets). All the studied sprays resulted in sub-100 nm particles in the overspray regardless of whether the product contained NMs or not. At least in some cases, these sub-100 nm particles consisted of condensed active ingredients. In pump sprays, water-based coating released 1.0×10^8 g^{-1} while the solvent based coating resulted in a 26 times higher emission (Göhler and Stintz, 2014).

2.5 Release from washing and leaching of textiles

NMs are usually added to textiles and fabrics by coating or by impregnating the textiles surfaces with NM by sorption, chemical binding of NM to the textile surface, or directly incorporating NM into textile fibers. Commonly studied textiles are cotton, PES, and PA6 and their mixtures including elastane, PBT, wool, nylon, PP, cellulose, spandex, elastic yarn, lycra or X-static fiber. The reviewed studies covered mainly NM release into washing water and artificial sweat, which were carried out by using commercially available textiles, plush toys, towels, shirts, surgical cloths and medical masks containing Ag, TiO_2 , or Ag and TiO_2 NMs (Table S5). The NM release from textiles is expressed as mg of NM per kg or per m^2 of textile. The released mass, if needed, was calculated from concentration and volume of immersion fluid. The amount of release NM may depend on their initial mass concentration, $m_{\text{NM},0}$, NM addition technique, textile/fabric type, leaching suspension, and environmental conditions. Here we report NM released mass, $m_{\text{NM,released}}$, as fraction of $m_{\text{NM},0}$, which allows for inter-comparison of different studies (Figure 5).

The release of NM changes with consecutive washings or artificial sweat immersions until all NM is released (Benn and Westerhoff, 2008; Lorenz *et al.*, 2012). Mitrano *et al.* (2015b) showed that the washing detergent and number of washing cycles has an effect on the morphology of the released particles. Kulthong *et al.* (2010) measured release ratios exceeding 100% in artificial sweat, which suggests that these results are not reliable (Table S14). However, both Kulthong *et al.* (2010) and Von Goetz *et al.* (2010) found that Ag NM release strongly depends on the composition of the artificial sweat solution (Figure 5). Guiot *et al.* (2009) also studied airborne particle emission rates during mechanical abrasion of a fabric consisting of PET and PVC coated with MMT. They found that released particles were mainly below 100 nm in diameter for PET and PVC with and without MMT.

First wash and rinse of textiles containing Ag NM released 0.5 to 35% of the initial elemental Ag concentration (Figure 5). The Ag is released mainly in ionic form (dissolved) and as precipitates such as AgCl and Ag associated with S, Si, and O but is also released as metallic Ag particles (Benn and Westerhoff, 2008; Benn *et al.*, 2010; Lorenz *et al.*, 2012; Pasricha *et al.*, 2012; Quadros *et al.*, 2013; Von Goetz *et al.*, 2013; Mitrano *et al.*, 2014). First wash and rinse of textiles containing TiO₂ NM released 0.01 to 3.4 % of the initial elemental Ti concentration as TiO₂ agglomerates. Figure 5 suggest that the type of textile or NM incorporation technique did not make any difference on the Ag or Ti release fraction. Release of Ag and Ti from fabrics to artificial sweat solutions (ISO 105-E04, 2008) is on average between 1.2 and 3.4 times lower than to wash water during laundry. Washing and rinsing of TiO₂ NM textiles and leaching to artificial sweats released TiO₂ NM agglomerates with sizes ranging from *ca.* 60 nm to over 450 nm in diameter (Von Goetz *et al.*, 2013; Mitrano *et al.*, 2014; Kulthong *et al.*, 2010).

2.6 Release from incineration

At the end-of-life, some of the nano-products will be incinerated together with other municipal waste in a waste incineration plant at up to 1400 °C (Walser *et al.* 2012). During incineration is formed airborne

particulate matter (fly ash) and solid combustion residues (slag). Slag is cooled with slag water and the exhaust gas is scrubbed before released to the atmosphere. Slag water and water from the scrubber are released to waste water stream. Incineration studies reported particulate matter release or residue from Incineration as a weight fraction of initial mass.

Rodes *et al.* (2011) studied under different ventilation conditions incineration of PA6 and PP containing fire retardants, nanoclay, and both fire retardants and nanoclay. It was found that in PA6 additives did not effect on the particle size distribution but changed the soot production yield and for PP additives determine the particle size of the soot. Under fully developed flame at 825 °C and at feed rate of 1 g·min⁻¹ the mass yield varied from 1.2 to 2.9 wt.% for PA6 and from 1.0 to 4.4 wt.% for PP.

Walser *et al.* (2012) sprayed at the waste incineration plant 8140 g nano-CeO₂ to municipal solid waste and 814 g nano-CeO₂ directly to the furnace representing worst case scenario. After incineration of waste sprayed with CeO₂, from initial CeO₂ mass they detect 32, 7, 0.009 and 0 wt.% from slag, fly ash, fly ash treatment and clean gas, respectively. When the CeO₂ was directly sprayed to the flame the mass fractions were 18, 15, 0.58, 5.6×10⁻⁵ wt.% for slag, fly ash, fly ash treatment and clean gas, respectively. Free and agglomerated CeO₂ nanoparticles were detected. The waste incinerator plant exhaust air filtration efficiency was >99. 6% for CeO₂ particles.

Chivas-Joly *et al.* (2014) studied incineration of PA6 containing 0 (reference), 0.2, and 1 wt.% CNTs and PMMA containing CNTs at the same concentrations as PA6 using calorimeters. At a heat flux of 50 kW m⁻² the aerosol mass yield varied from 0.39 to 0.63 wt.% for PA6 and from 0.37 to 0.46 wt.% for PMMA. The CNTs did not effect on airborne particles mass size distribution in PA6 but the PMMA containing CNTs reduced particle emissions in the size range from 0.6 to 2.5 µm. From PA6 containing CNTs, free CNTs were found from particles below the aerodynamic diameter of 30 nm.

Ounoughene *et al.* (2015) studied incineration of PA6 containing 0 (reference), 1, and 5 wt.% HNTs at 850 °C. Airborne particles and residual ash consisted of soot particles and mineral particles and agglomerates

transformed from HNTs. Thermogravimetric analysis showed that HNTs are first dehydrated at *ca.* 200 °C, and PA6 mass is lost between 300 to 500 °C, after which HNTs are dehydroxylated at *ca.* 500 to 900 °C and deformations occurs from 1200 to 1400 °C. Combustion reduces HNTs mass by 14 wt.% from its initial mass due to water release.

Sotiriou *et al.* (2015) who studied thermal decomposition of PU containing 0.09 wt.% CNTs at 500 and 800 °C. They did not detect CNTs from aerosol at any temperature. Incineration at 500 °C produced residual ash where they could detect CNTs protruding from the ash particles at concentration of 1.62 wt.% which correspond close to the initial mass of CNTs added in PU. This is in line with Vilar *et al.* (2011) who found that CNTs can be recovered from PA6 for re-use purposes using calcination at 410 °C. At 800 °C PU was combusted completely and they could not detect residual ash.

Sotiriou *et al.* (2016) studied thermal decomposition of PU containing 0.09 wt.% CB and 0.09 wt.% CNT and PE containing 4 wt.% Fe₂O₃ and 2 wt.% Organic pigment Red 254 and their references at up to 500 °C and 800 °C by analyzing airborne particles and residual ash. In thermal decomposition aerosol was released mainly as <100 nm particles where total yield ranged from 2.09 to 7.74 wt.% at 500 °C and 3.06 to 6.71 wt.% at 800 °C. They found only Fe₂O₃ filler particles from released aerosol and the release characteristic is dictated by the matrix and not nanofillers. Amount of residual ash varied at 500 °C incineration varied from 0.9 to 5 wt.% consisting mainly of EC from 75 to 84.9 % and OC except PE containing Fe₂O₃ consisted only Fe₂O₃. From the residual ash particles surface was detected filler particles. Residual ash at 800 °C incineration of PU and PE containing organic fillers were below detection limits but Fe₂O₃ filler remained at yield of 3.9 wt.%.

Incineration studies involve temperatures over 500 °C in which matrix is combusted and airborne soot particles and ash is produced. Depending on the temperatures and materials NM is deformed (*e.g.* HNTs; Ounoughene *et al.*, 2015) or may be recovered from the matrix (*e.g.* CNTs; Sotiriou *et al.* 2015, 2016; Vilar *et al.* 2011). NM additives may determine the emission yield and effect on the particle size distribution as

shown for PP nanocomposites (Rodes *et al.* 2011) and PMMA containing CNTs (Chivas-Joly *et al.* 2014) but it may be also determined by the matrix only as shown for PA6 nanocomposites (Rodes *et al.* 2011; Chivas-Joly *et al.* 2014) and PU and PE nanocomposites by Sotiriou *et al.* (2016). Reminders of NM additives from incomplete combustion are mainly found from residual ash (Vilar *et al.* 2011; Chivas-Joly *et al.* 2014; Ounoughene *et al.* 2015; Sotiriou *et al.* 2015; 2016) but may be found from aerosol in small fractions (Chivas-Joly *et al.* 2014; Sotiriou *et al.* 2016). Waste incineration plant filtering system is efficient >99.6 % so the main environmental risk is related to treatment of slug and quenching water (Walser *et al.*, 2012). The residual masses from incineration processes are shown in Table S15.

2.7 Other articles

The “Other articles” group covers studies which do not fall into any of the above categories. These studies examine how NMs can be used in cements (Wohlleben *et al.*, 2011; Hirth *et al.*, 2013; Van Broekhuizen *et al.*, 2011) ceramics (Van Broekhuizen *et al.*, 2011; Ren and Smith, 2013), dental composites (Moreau *et al.*, 2012), and laser printer toners (Pirela *et al.*, 2014) (Table S6, SI). In addition, Farkas *et al.* (2011) showed how a commercial laundry machine designed to produce Ag NM to washing water effluent increased the effluent Ag concentration by $11 \mu\text{g Ag}\cdot\text{L}^{-1}$, where Ag was detected both in ionic form and particulate form with mean diameter of 10 nm. The Ag concentrations in washed cotton fabrics were similar to the levels found in the laundry machine effluent. A two year aging study of dental composites containing 0 to 20% $\text{Ca}_3[\text{PO}_4]_2$ NM including mechanical abrasion and leaching to water at different temperatures, did not show any material release or visible damage on the analyzed surfaces (Moreau *et al.*, 2012). Bielefeldt *et al.* (2013) measured release from ceramic plates containing 0.72 to $7.2 \mu\text{g}\cdot\text{cm}^{-2}$ nano-Ag, varying from 20 to 83%, to ultrapure water and NaOCl solution, respectively. Laser printer toner contains various organic and elemental carbons and metal/metal oxide NMs, which become airborne and respirable during printing which depend on the printer type (Pirela *et al.*, 2014).

Our review on the "Other articles" group shows that the release or emission rate assessment may require unique procedures, and in some cases, needs to be monitored *in situ* as Walser *et al.* (2012) studied CeO₂ mass flows in a waste incineration plant.

3. Examples of exposure assessment modelings

Here we give to examples how to use the quantitative release rate for personal exposure assessment in case of sanding and environmental exposure assessment in case of washing laundry.

3.1 Removing paint from wood boards by sanding

In this exposure scenario, a wooden board painted with a paint containing Nano Amor and NaBond TiO₂ rutile nanoparticles 36 wt.% (Paint 2 in Gomez *et al.* 2014) is sanded using a Metabo FSR200 hand-held sanding machine where the dust collector cartridge was removed (user modified) and equipped with a sanding paper with a grit size of 120. This is the worst exposure scenario what can be obtained using this kind of setup and the process corresponds to sanding test performed by Gomez *et al.* (2014). We assume that 10 g of paint is sanded in a 20 m³ room without ventilation and the total exposure time is 120 minutes which are the same conditions as in Mackevica and Hansen (2016).

Because Gomez *et al.* (2014) did not give the MRR we measured that by sanding painted wooden boards using the same sanding system. Because the same paint (Paint 2 in Gomez *et al.*, 2014) was not available we measured MRRs from wooden boards which were coated with paints containing ~10 wet wt.% Nano-silica sol and 10 wet wt.% UV titan (G3A and G2B in Koponen *et al.* (2011), respectively). The measured MRRs were 3.0 and 0.9 g·min⁻¹ for G3A and G2B, respectively. Here we used the MRR of 0.9 g·min⁻¹ and thus the sanding time to remove 10 g of paint is 638 seconds.

Mass emission rates from the sanding were calculated from particle number size distributions (Figure 6 Paint 2 in Gomez *et al.* (2014) and here Figure 6a) by assuming spherical particles. Density of particles was assumed to be composed 36% of TiO₂ rutile bulk density of 4.23 g·cm⁻³ and 64% of paint additives density of 1 g·cm⁻³. This results to a density of 2.16 g·cm⁻³. The emission rate distribution includes emissions from sanding machine which influence on mass emission rate is < 0.001 %. Figure S2a shows that ~75 % of the mass was measured by three highest ELPI channels ($D_{pg} > 3 \mu\text{m}$). In some studies, the ELPI have shown to overestimate large particles particle concentrations due to reduced sensitivity in the upper stages (Pagels *et al.*, 2005; Jensen *et al.*, 2015).

The air exchange ratio was assessed from the particle number concentration decay using the mass balance of indoor aerosol particles (*e.g.* Hussein and Kulmala, 2008). The mass balance of aerosol particles inside a room without ventilation can be described without coagulation as

$$\frac{dm(t)}{dt} = \frac{S_m(t)}{V} - \beta \times m(t), \quad (2)$$

where m [$\text{mg}\cdot\text{m}^{-3}$] is the mass concentration, t [s] is time, S [$\text{cm}^{-3}\cdot\text{s}^{-1}$] is source of particles, V [m^3] is volume of the room, and β [s^{-1}] is the deposition rate of particles onto surfaces. For comparison of the results with Mackevica and Hansen (2016), The modelings were made by assuming the deposition rate to be 0 s^{-1} (without deposition) or by using a deposition rate estimated for an empty 20 m^3 cubic room having smooth surfaces with a friction velocity of $1 \text{ cm}\cdot\text{s}^{-1}$ using a model developed by Lai and Nazaroff (2000). This result in deposition rates ranging from 0.004 h^{-1} to 5.6 h^{-1} for 73 nm and $8.1 \mu\text{m}$ particles, respectively. Typical deposition rates for $8 \mu\text{m}$ particles vary from ~ 1.7 to 7 (Hussein and Kulmala, 2008). Friction velocity effects mainly deposition of $<3 \mu\text{m}$ particles (Hussein and Kulmala, 2008). Thus, correct friction velocity is not critical for this case where particles $>3 \mu\text{m}$ in diameter accounts for majority of the mass in the air.

The modeling's shows that mass concentrations increase at the maximum at the end of sanding. If there are no sinks for the mass concentrations the mass concentration remains at the maximum level at $217 \text{ mg}\cdot\text{m}^{-3}$ (Figure 6b). This correspond to mass of 4.3 g in the room air which is high considering that most of the sanding dust is beyond the ELPI measurement size range of $10 \mu\text{m}$ or non-airborne dust. If we take into account deposition of particles to the surfaces the mass concentration peak after sanding is $184 \text{ mg}\cdot\text{m}^{-2}$ after which the concentration decays mainly due to gravitational settling of particles $> 1 \mu\text{m}$ in diameter (Figure 6c). Average concentrations during the exposure time were $207 \text{ mg}\cdot\text{m}^{-3}$ without particle losses and $86 \text{ mg}\cdot\text{m}^{-3}$ when particle deposition was taken into account.

Inhaled dose during 2 hour exposure can be estimated from the size resolved particle mass distributions. Here we assumed that the respiratory minute volume (minute ventilation of the lungs) corresponds to light exercise ($25 \text{ L}\cdot\text{min}^{-1}$) breathing and the total deposition fractions during inspiration and expiration was estimated using simplified deposition fraction equations for the ICRP model (ICRP, 1994) as described by Hinds (1999). The method provides a first approximation to estimate magnitude of the total deposited dose (see *e.g.* Koivisto *et al.* 2012). During 2 hour exposure total amount of deposited mass is 520 mg without particle losses and 190 mg when particle deposition was taken into account. This corresponds for 60 kg person doses of 8.7 and $3.2 \text{ mg}\cdot\text{kg}^{-1}$, respectively and the TiO_2 dose would be 36% of the total dose *e.g.* 3.2 and $1.1 \text{ mg}\cdot\text{kg}^{-1}$, respectively, if we assume TiO_2 particle number concentrations distributed uniformly in each size class.

In the same exposure scenario, the body weighted TiO₂ dose would be 40 mg kg⁻¹ according to the ECHA R.15 exposure and dose model (Mackevica and Hansen, 2016). Here, the body weighted doses were 13 and 36 times smaller depending if there were no concentration sinks or assuming gravitational settling as sink for concentrations. It must be noted that in a small room without ventilation human breathing has significant effect on the concentrations. For example, in this example case without taking particle deposition into account, human breathing removed 12 % of mass from the room air. In the ECHA R.15 exposure and dose model the TiO₂ uptake via inhalation was 2.4 g during the 2 h exposure. Assuming 1 hour additional exposure time the dose would exceed available TiO₂ mass in the room.

In this example, main uncertainties in predicted mass concentrations were related to estimate of MRR and the mass emission rate that was converted from the particle number emission rates defined from the ELPI measurements.

3.2 Washing and rinsing 10 kg of PES textiles containing Ag

According to Geranio *et al.* (2009), a first time washing and rinsing of 10 kg PES incorporated with 99 mg·kg⁻¹ Ag would release 1.3% of the Ag to the washing water which corresponds to release of 13 mg Ag (Figure 5). If the amount of Ag is increased to 390 mg·kg⁻¹, the release fraction increases to 17 %, which would result to release of 663 mg Ag (Figure 5). If one uses 20 liters water for washing and rinsing the average Ag concentration for the water would be 0.65 mg·L⁻¹ and 33 mg·L⁻¹, respectively. The Ag is released mainly in ionic form (dissolved) and precipitates as AgCl and Ag/S but also as metallic Ag particles (Benn and Westerhoff, 2008; Benn *et al.*, 2010; Lorenz *et al.*, 2012; Pasricha *et al.*, 2012; Quadros *et al.*, 2013; Von Goetz *et al.*, 2013; Mitrano *et al.*, 2014). It must be noted that the washing detergent as well as the type of wash cycles has an effect on the amount released and type of released fragments (Mitrano *et al.*, 2015).

4. Concluding remarks and future prospects

In this work, we were able to extract properties of released fragments from 60 studies and quantitative release characteristics from 36 scientific publications providing a total of 374 different release scenarios. The quantitative releases are presented in Figures 1-5 and Tables S10-S15 and released particle characteristics in Tables S1-S6. Our data-library is the first step towards a general NM-product and article

release library. To demonstrate the potential use of the release data, we have given two examples on how to predict exposure concentrations showing that process specific emission rates, and in this cases also information on size-distribution, are crucial for detailed modelling-based exposure assessments. In short, Supporting Information is used to identify the study mimicking exposure scenario. Then, if exposure study is available, type of the released fragments are listed in Tables S1-S6 and quantitative releases can be found from Figures 1-5 or Tables S10-S15.

The library presented in this study is lacking explicit uncertainties and variations in quantitative releases and does not contain information on size-distributions of the emitted materials. Here, we assume that the experimental setup does not result in losses (*e.g.* deposition, sampling efficiency, full mixing of concentrations) nor has any influence on the release characteristics (*e.g.* coagulation, flocculation). In future investigations, these processes should be taken into account as *e.g.* in Gomez *et al.* (2014). In washing and leaching studies, the morphology of released material and their by-products should be assessed as done *e.g.* by Mitrano *et al.* (2014). We recommend that future release measurements should provide information on:

- Properties of the matrix and added NM, NM addition technique, concentration, and level of NM dispersion in the matrix.
- Release scenario and process parameters.
- Concentration gradients in the sampling volume (fully mixed concentrations are preferred unless it influences on release characteristics).
- The influence of the setups on the concentrations (*e.g.* deposition, coagulation, flocculation, chemical reactions, sampling efficiency).
- The morphologies of the released fragments and transformation products due to aging (Dwivedi *et al.*, 2015; Mitrano *et al.*, 2015a; 2015b).

- In mechanical processes process rate or MRR. The MRR can be used to calculate process times and estimate environmental exposure and personal exposure (*e.g.* dermal exposure).
- Size-distribution concentration data, which for airborne particle should include at least the 10 nm to *ca.* 10 μm aerodynamic size-range. The concentrations of particles between *ca.* 1 to 10 nm should be measured to assess the particle concentrations in the size-overlap between gas phase compounds and airborne particles (see *e.g.* Pedata *et al.* (2015) about concern related to sub-10 nm particle emissions).
- Effective density to convert particle number size distributions to particle mass distributions.
- Concentration of gas phase compounds including VOCs, when relevant.
- Uncertainties and variations of quantitative releases.

Currently, there is no general guidance available to measure quantitative release from various release scenarios. Harmonized methods would reduce systematic errors (*e.g.* mixing of concentrations in atmospheric measurements) and make the release results comparable. Mass balance should be reported *i.e.* from the removed fraction which is released as particulate matter, dissolved fraction, vapors, or transferred to other solid compounds. Properties of released fragments should be analyzed with systematic techniques and fraction of free or accessible NMs should be defined *e.g.* using labelled NMs or automatized EM analysis. Currently, in regulatory exposure assessment it is usually assumed that NM is released as in pristine form which is far from reality (*e.g.* Schlagenhauf *et al.*, 2015).

We propose to mimic the stress scenario by following standardized stress test procedures or simulate the process in environmentally relevant and well-controlled conditions. Sampling of released fragments should be harmonized so that it can be linked to hazard assessment and further risk assessment. For example, the release R_p depend on sampling technique (*e.g.* non-volatile fraction, particles in specific size range) which why different measurements are not always directly comparable. Also, particle number emission rates alone cannot be used to estimate mass flows or linked to hazard. Without systematic experimental

methods, it is challenging to understand how NM additives modulate the potential release, when different stress factors are applied. This is also essential for understanding potential hazards associated with potential exposure to the released materials.

Acknowledgement

This work was made with contribution by Dr. Samuel Brunner from Empa, Swiss Federal Laboratories for Materials Science and Technology, Laboratory for Building Energy Materials and Components. The research leading to these results has received funding from the European Union Seventh Framework Programme [FP7/2007-2013] under EC-GA No. 604305 'SUN', a grant from the Danish Environmental Protection Agency, and by a grant from the Danish Centre for Nanosafety (grant agreement no. 20110092173/3) by the Danish Working Environment Research Fund.

Appendix A. Supporting Information: Tables summarizing study designs and emission characteristics.

Supporting Information to this article can be found online at XXX.

References

Al-Kattan, A., Wichser, A., Vonbank, R., Brunner, S., Ulrich, A., Zuin, S., Nowack, B., 2013. Release of TiO₂ from paints containing pigment-TiO₂ or nano-TiO₂ by weathering. *Environ. Sci.: Process Impacts* 15, 2186–2193.

Al-Kattan, A., Wichser, A., Vonbank, R., Brunner, S., Ulrich, A., Zuin, S., Arroyo, Y., Golanski, L., Nowack, B., 2015. Characterization of materials released into water from paint containing nano-SiO₂. *Chemosphere* 119, 1314–1321.

- Bekker, C., Brouwer, D. H., van Duuren-Stuurman, B., Tuinman, I. L., Tromp, P., Fransman, W., 2014. Airborne manufactured nano-objects released from commercially available spray products: temporal and spatial influences. *J. Expo. Sci. Environ. Epidemiol.* 24, 74–81.
- Benn, T., Cavanagh, B., Hristovski, K., Posner, J., Westerhoff, P., 2010. The release of nanosilver from consumer products used in the home. *J. Environ. Qual.* 39, 1875–1882.
- Benn, T., Westerhoff, P., 2008. Nanoparticle silver released into water from commercially available sock fabrics. *Environ. Sci. Technol.* 42, 4133–4139.
- Bernard, C., Nguyen, T., Pellegrin, B., Holbrook, R., Zhao, M., Chin, J., 2011. Fate of graphene in polymer nanocomposite exposed to UV radiation. *J. Phys.: Conf. Ser.* 304:012063.
- Bielefeldt, A., Stewart, M., Mansfield, E., Summers, R. S., Ryan, J., 2013. Effects of chlorine and other water quality parameters on the release of silver nanoparticles from ceramic surface. *Water Res.* 47, 4032–4039.
- Busquets-Fité, M., Fernandez, E., Janer, G., Vilar, G., Vázquez-Campos, S., Zanasca, R., Citterio, C., Mercante, L., Puentes, V., 2013. Exploring release and recovery of nanomaterials from commercial polymeric nanocomposites. *J. Phys.: Conf. Ser.* 429:012048.
- Caballero-Guzman, A., Nowack, B., 2016. A critical review of engineered nanomaterial release data: Are current data useful for material flow modeling? *Environ Pollut.* 213, 502-517.
- Chen, B. T., Afshari, A., Stone, S., Jackson, M., Schwegler-Berry, D., Frazer, D. G., Castranova, V., Thomas, T. A., 2010. Nanoparticles-containing spray can aerosol: characterization, exposure assessment, and generator design. *Inhal. Toxicol.* 22, 1072–1082.

- Chin, J., Byrd, E., Embree, N., Garver, J., Dickens, B., Finn, T., Martin J., 2004. Accelerated UV weathering device based on integrating sphere technology. *Rev. Sci. Instrum.* 75, 4951-4959.
- Chivas-Joly, C., Motzkus, C., Guillaume, E., Ducourtieux S., Saragoza, L., Lesenechal, D., Lopez-Cuesta, J-M., Longuet, C., Sonnier, R., Minisini B., 2014. Influence of carbon nanotubes on fire behaviour and aerosol emitted during combustion of thermoplastics. *Fire Mater.* 38, 46–62.
- Duncan, T.V., 2015. Release of Engineered Nanomaterials from Polymer Nanocomposites: the Effect of Matrix Degradation. *ACS Appl. Mater. Interfaces* 7, 20–39.
- Duncan, T.V., Pillai K., 2015. Release of Engineered Nanomaterials from Polymer Nanocomposites: Diffusion, Dissolution, and Desorption. *ACS Appl. Mater. Interfaces* 7, 2–19.
- Dwivedi, A. D., Dubey, S. P., Sillanpää, M., Kwon, Y-N., Lee, C., Varma, R. S., 2015. Fate of engineered nanoparticles: Implications in the environment. *Coord. Chem. Rev.* 287, 64–78.
- Farkas, J., Peter, H., Christian, P., Urrea, J. A. G., Hassellöv, M., Tuoriniemi, J., Gustafsson, S., Olsson, E., Hylland, K., Thomas, K. V., 2011. Characterization of the effluent from a nanosilver producing washing machine. *Environ. Int.* 37, 1057–1062.
- Fiorentino, B., Golanski, L., Guiot, A., Damlencourt, J-F., Boutry. D., 2015. Influence of paints formulations on nanoparticles release during their life cycle. *J. Nanopart. Res.* 17, 149.
- Flynn, M. R., Gatano, B. L., McKernan, J. L., Dunn, K. H., Blazicko, B. A., Carlton, G. N., 1999. Modeling Breathing-Zone Concentrations of Airborne Contaminants Generated During Compressed Air Spray Painting. *Ann. Occup. Hyg.* 32, 67-76.
- Fouvry, S., Liskiewicz, T., Kapsa, Ph., Hannel, S., Sauger, E., 2003. An energy description of wear mechanisms and its applications to oscillating sliding contacts. *Wear.* 255, 287–298.

- Franek, F., Badisch, E., Kirchgaßner, M., 2009. Advanced Methods for Characterisation of Abrasion/Erosion Resistance of Wear Protection Materials. *FME Transactions*. 37, 61-70.
- Froggett, S. J., Clancy, S. F., Boverhof, D. R., Canady, R. A., 2014. A review and perspective of existing research on the release of nanomaterials from solid nanocomposites. Part. *Fibre Toxicol.* 11:17.
- Ging, J., Tejerina-Anton, R., Ramakrishnan, G., Nielsen, M., Murphy, K., Gorham, J. M., Nguyen, T., Orlov, A., 2014. Development of a conceptual framework for evaluation of nanomaterials release from nanocomposites: Environmental and toxicological implications. *Sci. Total Environ.* 473–474, 9–19.
- Göhler, D., Nogowski, A., Fiala, P., Stintz, M., 2013. Nanoparticle release form nanocomposites due to mechanical treatment at two stages of the life-cycle. *J. Phys.: Conf. Ser.* 429:012045.
- Göhler, D., Stintz, M., Hillemann, L., Vorbau, M., 2010. Characterization of nanoparticle release from surface coatings by the simulation of a sanding process. *Ann. Occup. Hyg.* 54, 615–624.
- Göhler, D., Stintz, M., 2014. Granulometric characterization of airborne particulate release during spray application of nanoparticle-doped coatings. *J. Nanopart. Res.* 16:2520.
- Gomez, V., Levin, M., Saber, A. T., Irusta, S., Maso, M.D., Hanoi, R., Santamaria, J., Jensen, K.A., Wallin, H., Koponen, I.K., 2014. Comparison of dust release from epoxy and paint nanocomposites and conventional products during sanding and sawing. *Ann. Occup. Hyg.* 58, 983–994.
- Grassian, V.H., Haes, A.J., Mudunkotuwa, I.A., Demokritou, P., Kane, A.B., Murphy, C.J, Hutchison, J.E., Isaacs, J.A., Jun, Y.-S., Karn, B., Khondaker, S.I., Larsen, S.C.M, Lau, B.L.T, Pettibone, J.M., Sadik, O.A., Salehm, N.B., Teaguen C., 2016. NanoEHS – defining fundamental science needs: no easy feat when the simple itself is complex. *Environ. Sci.* 3, 15-27.

Guiot, A., Golanski, L., Tardif, F., 2009. Measurement of nanoparticle removal by machining. *J. Phys.: Conf. Ser.* 170:012014.

Hagendorfer, H., Lorenz, C., Kaegi, R., Sinnet, B., Gehrig, R., Goetz, N. V., Scheringer, M., Ludwig, C., Ulrich, A., 2010. Size-fractionated characterization and quantification of nanoparticle release rates from a consumer spray product containing engineered nanoparticles. *J. Nanopart. Res.* 12, 2481–2494.

Harper, S., Wohlleben, W., Doa, M., Nowack, B., Clancy, S., Canady, R., Maynard, A., 2015. Measuring Nanomaterial Release from Carbon Nanotube Composites: Review of the State of the Science. *J. Phys.: Conf. Ser.* 617:012026.

Hinds, W. C., 1999. Ed. *Aerosol Technology: Properties, Behavior, and Measurement of Airborne Particles*, Wiley: New York, pp 233-259.

Hirth, S., Cena, L., Cox, G., Tomovic, Z., Peters, T., Wohlleben, W., 2013. Scenarios and methods that induce protruding or released CNTs after degradation of nanocomposite materials. *J. Nanopart. Res.* 15, 1504.

Hsu, L., Chein, H., 2007. Evaluation of nanoparticles emission for TiO₂ nanopowder coating materials. *J. Nanopart. Res.* 9:157–163.

Huang, G., Park, J., Cena, L., Shelton, B., Peters, T., 2012. Evaluation of airborne particle emissions from commercial products containing carbon nanotubes. *J. Nanopart. Res.* 14:1231.

Hussein, T., Kulmala, M., 2008. *Indoor aerosol modeling: basic principles and practical applications*. *Water Air Soil Poll.* 8, 23-34.

ISO 7784-2, 2006. *Paint and varnish—determination of resistance to abrasion. Part 2: rotating abrasive rubber wheel method*. International Organization for Standardization, Geneva.

ISO 11507, 2007. Paints and varnishes: exposure of coatings to artificial weathering: exposure to fluorescent UV lamps and water. International Organization for Standardization, Geneva.

ISO 4892-2, 2013. Plastics – Methods of exposure to laboratory light sources Part 2:

Xenon-Arc Lamps. International Organization for Standardization, Geneva.

ISO 105-E04, 2008. Textiles - Tests for colour fastness - Part E04: Colour fastness to perspiration.

International Organization for Standardization, Geneva.

Jensen, A.C.Ø., Levin, M., Koivisto, A.J., Kling, K.I., Saber, A.T., Koponen, I.K., 2015. Exposure Assessment of Particulate Matter from Abrasive Treatment of Carbon and Glass Fibre-Reinforced Epoxy-Composites – Two Case Studies. *Aerosol Air Qual. Res.* 15: 1906–1916.

Juganson, K., Ivask, A., Bilnova, I., Mortimer, M., Karhu, A. NanoE-Tox: New and in-depth database concerning ecotoxicity of nanomaterials. *Beilstein J. Nanotechnol.* 2015, 6, 1788–1804.

Kingston, C., Zepp, R., Andrady, A., Boverhof, D., Fehir, R., Hawkins, D., Roberts, J., Sayre, P., Shelton, B., Sultani, Y., Vejinsj, V., Wohlleben W., 2014. Release characteristics of selected carbon nanotube polymer composites. *Carbon* 68, 33-57.

Koivisto, A.J., Aromaa, M., Mäkelä, J.M., Pasanen, P., Hussein, T., Hämeri, K., 2012. Concept to estimate regional inhalation dose of industrially synthesized nanoparticles. *ACS Nano* 6, 1195-1203.

Koivisto, A.J., Yu, M., Hämeri, K., Seipenbusch, M., 2012. Size resolved particle emission rates from an evolving indoor aerosol system. *J. Aerosol Sci.* 47:58-69.

Koponen, I. K., Jensen, K. A., Schneider, T., 2011. Comparison of dust released from sanding conventional and nanoparticle doped wall and wood coatings. *J. Expo. Sci. Environ. Epidemiol.* 21, 408–418.

- Kulthong, K., Srisung, S., Boonpavanitchakul, K., Kangwansupamonkon, W., Maniratanachote, R., 2010. Determination of silver nanoparticle release from antibacterial fabrics into artificial sweat. Part. Fibre Toxicol. 7, 8.
- Lai, A.C.K., Nazaroff, W.W., 2000. Modeling indoor particle deposition from turbulent flow onto smooth surfaces. J. Aerosol Sci. 31, 463-476.
- Le Bihan, O., Shandilya, N., Gheerardyn, L., Guillon, O., Dore, E., Morgenev, M., 2013. Investigation of the release of particles from a nanocoated product. Adv. Nanopart. 2, 39-44.
- Li, W., Kara, S., 2011. An empirical model for predicting energy consumption of manufacturing processes: a case of turning process. Proc. IMechE Vol. 225 Part B: J. Engineering Manufacture. 225, 1636-1646.
- Lorenz, C., Hagendorfer, H., von Goetz, N., Kaegi, R., Gehrig, R., Ulrich, A., Scheringer, M., Hungerbühler, K., 2011. Nanosized aerosols from consumer sprays: experimental analysis and exposure modeling for four commercial products. J. Nanopart. Res. 13:3377-3391.
- Lorenz, C., Windler, L., von Goetz, N., Lehmann, R., Schuppler, M., Hungerbühler, K., Heuberger, M., Nowack, B., 2012. Characterization of silver release from commercially available functional (nano) textiles. Chemosphere. 89, 817-24.
- Losert, S., von Goetz, N., Bekker, C., Fransman, W., Wijnhoven, S. W. P., Delmaar, C., Hungerbühler, K., Ulrich, A., 2014. Human Exposure to Conventional and Nanoparticle-Containing Sprays - A Critical Review. Environ. Sci. Technol. 48, 5366-5378.
- Lv, Y., Huang, Y., Yang, J., Kong, M., Zhao, J., Li, G., 2015. Outdoor and accelerated laboratory weathering of polypropylene: A comparison and correlation study. Polym. Degrad. Stab. 112, 145-159.

Mackevica, A., Hansen, S., 2016. Release of nanomaterials from solid nanocomposites and consumer exposure assessment – a forward-looking review. *Nanotoxicol.* 10:641-653.

Martin, J.W., Chin, J.W., Nguyen T., 2003. Reciprocity law experiments in polymeric photodegradation: a critical review. *Prog. Org. Coat.* 47, 292-311.

Massarsky, A., Trudeau, V.L., Moon, T.W., 2014. Predicting the environmental impact of nanosilver. *Environ. Toxicol. Phar.* 38, 861-873.

Met Office, 2007. National Meteorological Library and Archive, Fact sheet No. 6 – The Beaufort Scale. <http://www.metoffice.gov.uk>, accessed 13 December 2016.

Mitrano, D. M., Dasilva. Y. A. R., Nowack, B., 2015b. Effect of Variations of Washing Solution Chemistry on Nanomaterial Physicochemical Changes in the Laundry Cycle. *Environ. Sci. Technol.* 49, 9665–9673.

Mitrano, D. M., Motellier, S., Clavaguera, S., Nowack, B. 2015a. Review of nanomaterial aging and transformations through the life cycle of nano-enhanced products. *Environ Int.* 77, 132–147.

Mitrano, D. M., Rimmelé, E., Wichser, A., Height, M., Nowack, B., 2014. Presence of Nanoparticles in Wash Water from Conventional Silver and Nano-silver Textiles. *ACS Nano* 8, 7208-7219.

Moreau, J., Weir, M., Giuseppetti, A., Chow, L., Antonucci, J., Xu, H., 2012. Long-term mechanical durability of dental nanocomposites containing amorphous calcium phosphate nanoparticles. *J Biomed Mater Res Part B: Appl. Biomater.* 100, 1264–1273.

Morgeneyer, M., Shandilya, N., Chen, Y-M., Le Bihan, O., 2015. Use of a modified Taber abrasion apparatus for investigating the complete stress state during abrasion and in-process wear particle aerosol generation. *Chem. Eng. Res. Des.* 93, 251-256.

Nazarenko, Y., Han, T., Liroy, P. J., Mainelis, G., 2011. Potential for exposure to engineered nanoparticles from nanotechnology-based consumer spray products. *J. Expo. Sci. Environ. Epidemiol.* 21, 515–528.

Nazarenko, Y., Han, T., Liroy, P. J., Mainelis, G., 2014. Quantitative assessment of inhalation exposure and deposited dose of aerosol from nanotechnology-based consumer sprays. *Environ. Sci. Nano* 1, 161–171.

Nguyen, T., Pellegrin, B., Bernard, C., Gu, X., Gorham, J. M., Stutzman, P., Stanley, D., Shapiro, A., Byrd, E., Hettenhouser, R., Chin, J., 2011. Fate of nanoparticles during life cycle of polymer nanocomposites. *J. Phys.: Conf. Ser.* 304:012060.

Nguyen, T., Pellegrin, B., Bernard, C., Rabb, S., Stutzman, P., Gorham, J., Gu, X., Yu, L., Chin, J., 2012. Characterization of surface accumulation and release of nanosilica during irradiation of polymer nanocomposites by ultraviolet light. *J. Nanosci. Nanotechnol.* 12, 6202–6215.

Nørgaard, A. W., Jensen, K. A., Janfelt, C., Lauritsen, F. R., Clausen, P. A., Wolkoff, P., 2009. Release of VOCs and particles during use of nanofilm spray Products. *Environ. Sci. Technol.* 43, 7824–7830.

Nowack, B., David, R.M., Fissan, H., Morris, H., Shatkin, J.A., Stintz, M., Zepp, R., Brouwer, D., 2013. Potential release scenarios for carbon nanotubes used in composites. *Environ. Int.* 59:1-11.

Nowack, B., Ranville, J.F., Diamond, S., Gallego-Urrea, J.A., Metcalfe, C, Rose J., Horne N., Koelmans, A.A., Klaine, S.J., 2012. Potential scenarios for nanomaterial release and subsequent alteration in the environment. *Environ. Toxicol. Chem.* 31, 50-59.

Ounoughene, G., Le Bihan, O., Chivas-Joly, C., Motzkus, C., Longuet, C., Debray, B., Joubert, A., Le Coq, L., Lopez-Cuesta, J.M., 2015. Behavior and Fate of Halloysite Nanotubes (HNTs) When Incinerating PA6/HNTs Nanocomposite. *Environ. Sci. Technol.* 49, 5450–5457.

Pagels, J., Gudmundsson, A., Gustavsson, E., Asking, L., Bohgard, M., 2005. Evaluation of Aerodynamic Particle Sizer and Electrical Low-Pressure Impactor for Unimodal and Bimodal Mass-Weighted Size Distributions. *Aerosol Sci. Technol.* 39, 871-887.

Pasricha, A., Jangra, S. L., Singh, N., Dilbaghi, N., Sood, K. N., Arora, K., Pasricha, R., 2012. Comparative study of leaching of silver nanoparticles from fabric and effective effluent treatment. *J. Environ. Sci.* 24, 852-859.

Pedata, P., Stoeger, T., Zimmermann, R., Peters, A., Oberdörster, G., D'Anna, A., 2015. "Are we forgetting the smallest, sub 10 nm combustion generated particles?" *Part Fib Toxicol.* 12, 34.

Petersen, E. J., Lam, T., Gorham, J. M., Scott, K. C., Long, C. J., Stanley, D., Sharma, R., Liddle, J. A., Pellegrin, B., Nguyen, T., 2014. Methods to assess the impact of UV irradiation on the surface chemistry and structure of multiwall carbon nanotube epoxy nanocomposites. *Carbon* 69, 194-205.

Pirela, S. V., Sotiriou, G. A., Bello, D., Shafer, M., Bunker, K. L., Castranova, V., Thomas, T., Demokritou, P., 2014. Consumer exposures to laser printer-emitted engineered nanoparticles: A case study of life-cycle implications from nano-enabled products. *Nanotoxicol.* 9:760-768.

Quadros, M. E., Marr, L. C., 2011. Silver nanoparticles and total aerosols emitted by nanotechnology-related consumer spray products. *Environ. Sci. Technol.* 45, 10713-10719.

Quadros, M. E., Pierson, R., Tulve, N. S., Willis, R., Rogers, K., Thomas, T. A., Marr, L. C., 2013. Release of silver from nanotechnology-based consumer products for children. *Environ. Sci. Technol.* 47, 8894-8901.

Rabb, S., Yu, L., Bernard, C., Nguyen, T., 2010. An Analytical Method to Quantify Silica Nanoparticles Accumulated on the Surface of Polymer Nanocomposites Exposed to UV Radiation. In *Proceedings of*

the NSTI-NanoTech.: June 21-24 2010. Edited by Taylor & Francis. Anaheim CA, 2010. ISBN 978-1-4398-3401-5.

Ren, D., Smith, J., 2013. Retention and transport of silver nanoparticles in a ceramic porous medium used for point-of-use water treatment. *Environ. Sci. Technol.* 47, 3825–3832.

Rhodes, J., Smith, C., Stec, A.A., 2011. Characterisation of soot particulates from fire retarded and nanocomposite materials, and their toxicological impact. *Polym. Degrad. Stab.* 96,277-284.

Robinson, J., Linder, A., Gemme, I. A., Poulsen, K. V., Burkhard, H., Högström, P., Linder, A., Burkhard, H., Kobilsek, M., Gemmel, A., 2011. In comparison of standard UV test methods for the ageing of cables, 60th IWCS conference, pp. 329-337, Charlotte, NC.

Saber, A.T., Jensen, K.A., Jacobsen, N.R., Birkedal, R., Mikkelsen, L., Møller, P., Loft, S., Wallin, H., Vogel U., 2012b. Inflammatory and genotoxic effects of nanoparticles designed for inclusion in paints and lacquers. *Nanotoxicol.* 6, 453-471.

Saber, A.T., Koponen, I.K., Jensen, K.A., Jacobsen, N.R., Mikkelsen, L., Møller, P., Loft, S., Vogel, U., Wallin, H., 2012a. Inflammatory and genotoxic effects of sanding dust generated from nanoparticle-containing paints and lacquers. *Nanotoxicol.* 6, 776–788.

Sachse, S., Silva, F., Zhu, H., Irfan, A., Leszczynska, A., Pielichowski, K., Ermini, V., Blazquez, M., Kuzmenko, O., Njuguna, J., 2012a. The effect of nanoclay on dust generation during drilling of PA6 nanocomposites. *J. Nanomater.* 2012:189386.

Sachse, S., Silva, F., Irfan, A., Zhu, H., Pielichowski, K., Leszczynska, A., Blazquez, M., Kazmina, O., Kuzmenko, O., Njuguna, J., 2012b. Physical characteristics of nanoparticles emitted during drilling of silica based polyamide 6 nanocomposites. *Conf. Ser. Mater. Sci. Eng.* 40:012012

- Schlagenhauf, L., Buerki-Thurnherr, T., Kuo, Y.-Y., Wichser, A., Nüesch, F., Wick, P., Wang, J., 2015. Carbon Nanotubes Released from an Epoxy-Based Nanocomposite: Quantification and Particle Toxicity. *Environ. Sci. Technol.* 49:10616–10623.
- Schlagenhauf, L., Nüesch, F., Wang J., 2014. Release of Carbon Nanotubes from Polymer Nanocomposites. *Fibers* 2, 108-127.
- Schripp, T., Wensing, M., Uhde, E., Salthammer, T., He, C., Morawska, L., 2008. Evaluation of ultrafine particle emissions from laser printers using emission test chambers. *Environ. Sci. Technol.* 42:4338-4343.
- Shandilya, N., Bihan, O. L., Bressot, C., Morgeneyer, M., 2015. Emission of titanium dioxide nanoparticles from building materials to the environment by wear and weather. *Environ. Sci. Technol.* 49, 2163–2170.
- Shandilya, N., Bihan, O. L., Bressot, C., Morgeneyer, M., 2014. Evaluation of the particle aerosolization from n-TiO₂ photocatalytic nanocoatings under abrasion. *J. Nanomater.* 1–11.
- Smulders, S., Luyts, K., Brabants, G., Van Landuyt, K., Kirschhock, C., Smolders, E., Golanski, L., Vanoirbeek, J., Hoet, P.H.M., 2014. Toxicity of Nanoparticles Embedded in Paints Compared with Pristine Nanoparticles in Mice. *Toxicol. Sci.* 141, 132-140.
- Sotiriou, G.A., Singh, D., Zhang, F., Chalbot, M.C., Spielman-Sun, E., Hoering, L., Kavouras, I.G., Lowry, G.V., Wohlleben, W., Demokritou, P., 2016. Thermal decomposition of nano-enabled thermoplastics: Possible environmental health and safety implications. *J. Hazard. Mater.* 305, 87-95.

Sotiriou, G.A., Singh, D., Zhang, F., Wohlleben, W., Chalbot, M.G., Kavouras, I.G., Demokritou, P., 2015. An integrated methodology for the assessment of environmental health implications during thermal decomposition of nano-enabled products. *Environ. Sci. Nano* 2, 262-272.

Srivastava, V., Gusain, D., Sharma, Y.C., 2015. Critical Review on the Toxicity of Some Widely Used Engineered Nanoparticles. *Ind. Eng. Chem. Res.* 54, 6209–6233.

Sung, L., Stanley, D., Gorham, J. M., Rabb, S., Gu, X., Yu, L. L., Nguyen, T., 2015. A quantitative study of nanoparticle release from nanocoatings exposed to UV radiation. *J. Coat. Technol. Res.* 12, 121–135.

Tan, Y-M., Flynn, M. R., 2002b. Methods for Estimating the Transfer Efficiency of a Compressed Air Spray Gun. *App. Occup. Environ. Hyg.* 17, 39-46.

Tan, Y-M., Flynn, M., Buller, T. S. A, 2002a. Field Evaluation of the Impact of Transfer Efficiency on Worker Exposure During Spray Painting. *Ann. Occup. Hyg.* 46, 103-112.

ICRP, 1994. Human Respiratory Tract Model for Radiological Protection. *Ann. The International Commission on Radiological Protection* 24: 1–482.

Tolaymat, T., El Badawy, A., Sequeira, R., Genaidy, A., 2015. An integrated science-based methodology to assess potential risks and implications of engineered nanomaterials. *J. Hazard. Mater.* 298,270-281.

Van Broekhuizen, P., Van Broekhuizen, F., Cornelissen, R., Reijnders, L., 2011. Use of nanomaterials in the European construction industry and some occupational health aspects thereof. *J. Nanopart. Res.* 13, 447–462.

Walser, T., Limbach, L.K., Brogioli, R., Erismann, E., Flamigni, L., Hattendorf, B., Juchli, M., Krumeich, F., Ludwig, C., Prikopsky, K., Rossier, M., Saner, D., Sigg, A., Hellweg, S., Günter, D., Stark, W.J., 2012.

Persistence of engineered nanoparticles in a municipal solid-waste incineration plant. *Nat. Nanotechnol.* 7, 520–524.

Vance, M.E., Kuiken, T., Vejerano, E.P., McGinnis, S. P., Hochella, Jr M.F., Rejeski, D., Hull, M S., 2015. Nanotechnology in the real world: Redeveloping the nanomaterial consumer products inventory. *Beilstein J. Nanotechnol.* 6, 1769–1780.

Vernez, D.S., Droz, P-O., Lazor-Blanchet, C., Jaques, S., 2004. Characterizing Emission and Breathing-Zone Concentrations Following Exposure Cases to Fluororesin-Based Waterproofing Spray Mists. *J. Occup. Environ. Hyg.* 1, 582–592.

Von Goetz, N., Lorenz, C., Windler, L., Nowack, B., Heuberger, M., Hungerbühler, K., 2013. Migration of Ag- and TiO₂ (nano) particles from textiles into artificial sweat under physical stress: Experiments and exposure modeling. *Environ. Sci. Technol.* 47, 9979–9987.

Vorbau, M., Hillemann, L., Stintz, M., 2009. Method for the characterization of the Machining induced nanoparticles release into air from surface coatings. *J. Aerosol. Sci.* 40, 209–217.

Windler, L., Lorenz, C., von Goetz, N., Hungerbühler, K., Amberg, M., Heuberger, M., Nowack, B., 2012. Release of titanium dioxide from textiles during washing. *Environ. Sci. Technol.* 46, 8181–8188.

Wohlleben, W., Brill, S., Meier, M., Mertler, M., Cox, G., Hirth, S., von Vacano, B., Strauss, V., Treumann, S., Wiench, K., Ma-Hock, L., Landsiedel, R., 2011. On the lifecycle of nanocomposites: comparing released fragments and their in-vivo hazards from three release mechanisms and four nanocomposites. *Small* 7, 2384–2395.

Wohlleben, W., Meyer, J., Muller, J., Müller, P., Vilsmeier, K., Stahlmecke, B., Kuhlbusch, T.A.J., 2016. Release from nanomaterials during their use phase: combined mechanical and chemical stresses

applied to simple and multi-filler nanocomposites mimicking wear of nano-reinforced tires. *Environ. Sci.: Nano* 3, 1036-1051.

Wohlleben, W., Neubauer N., 2016. Quantitative rates of release from weathered nanocomposites are determined across 5 orders of magnitude by the matrix, modulated by the embedded nanomaterial. *NanoImpact* 1, 39-45.

Wohlleben, W., Vilar, G., Fernández-Rosas, E., González-Gálvez, D., Gabriel, C., Hirth, S., Frechen, T., Stanley, D., Gorham, J., Sung, L-P., Hsueh, H-C., Chuang, Y-F., Nguyen, T., Vazquez-Campos, S., 2014. A pilot interlaboratory comparison of protocols that simulate aging of nanocomposites and detect released fragments. *Environ. Chem.* 11, 402-418.

Zuin, S., Gaiani, M., Ferrari, A., Golanski, L., 2014. Leaching of nanoparticles from experimental water-borne paints under laboratory test conditions. *J. Nanopart. Res.* 16, 2185.

SI references

ASTM D7309-11 Standard Test Method for Determining Flammability Characteristics of Plastics and Other Solid Materials Using Microscale Combustion Calorimetry.

Bello, D., Wardle, B. L., Yamamoto, N., De Villoria, R. G., Garcia, E. J., Hart, A. J., Ahn, K., Ellenbecker, M. J., Hallock, M., 2009. Exposure to nanoscale particles and fiber during Abrasion of hybrid advanced composites containing carbon nanotubes. *J. Nanopart. Res.* 11, 231–249.

Bello, D., Wardle, B. L., Zhang, J., Yamamoto, N., Santeufemio, C., Hallock, M., Virji, M. A., 2010. Characterization of exposures to nanoscale particles and fibers during solid core drilling of hybrid carbon nanotube advanced composites. *Int. J. Occup. Environ. Health.* 16, 434–450.

Bouillard, J. X., R'Mili, B., Moranviller, D., Vignes, A., Le Bihan, O., Ustache, A., Bomfim, J. A. S., Frejafon, E., Fleury, D., 2013. Nanosafety by design: risks from nanocomposite/nanowaste combustion. *J. Nanopart. Res.* 15, 1519–1530.

Cena, L., Peters, T., 2011. Characterization and control of airborne particles emitted during production of epoxy/carbon nanotube nanocomposites. *J. Occup. Environ. Hyg.* 8, 86–92.

European Organisation for Technical Approvals (EOTA). ETAG 004 – Guideline for European Technical Approval of External Thermal Insulation Composite Systems with Rendering. Edition March 2000, Brüssel. <http://www.eota.eu/en-GB/content/etags-used-as-ead/26/> (accessed on 17 Dec 2015).

Fransman, W., Bekker, C., Tromp, P., Duis, W.B., 2016. Potential Release of Manufactured Nano Objects During Sanding of Nano-Coated Wood Surfaces. *Ann. Occup. Hyg.*, doi:10.1093/annhyg/mew031.

Geranio, L., Heuberger, M., Nowack, B., 2009. The behavior of silver nanotextiles during washing. *Environ. Sci. Technol.* 43, 8113–8118.

Giraldo, L. F., Brostow, W., Devaux, E., López, B. L., Pérez, L.D., 2008. Scratch and Wear Resistance of Polyamide 6 Reinforced with Multiwall Carbon Nanotubes. *Journal of Nanoscience and Nanotechnology.* 8, 3176-3183.

Golanski, L., Gaborieau, A., Guiot, A., Uzu, G., Chatenet, J., Tardif, F., 2011. Characterization of machining-induced nanoparticle release from paints into liquids and air. *J. Phys.: Conf. Ser.* 304:012062.

Golanski, L., Guiot, A., Pras, M., Malarde, M., Tardif, F., 2012. Release-ability of nano fillers from different nanomaterials (toward the acceptability of nanoproduct). *J. Nanopart. Res.* 14:962.

Gorham, J., Nguyen, T., Bernard, C., Stanley, D., Holbrook, R., 2012. Photo-induced surface transformations of silica nanocomposites. *Surf. Interface. Anal.* 44, 1572–1581.

Hellmann, A., Schmidt, K., Ripperger, S., Berges, M., 2012. Release of ultrafine dusts during the machining of nanocomposites. *Gefahrst. Reinhalt. Luft.* 72, 473–476.

ISO 11341, 2004. Paints and varnishes – Artificial weathering and exposure to artificial radiation – Exposure to filtered xenon-arc radiation. International Organization for Standardization, Geneva.

ISO 3892–2, 2006. Plastics – Methods of exposure to laboratory light sources. International Organization for Standardization, Geneva.

ISO 5660-1:2002: Reaction to fire tests – heat release, smoke production and mass loss rate – part 1: heat release rate (cone calorimeter method). International Organization for Standardization, Geneva.

Irfan, A., Sachse, S., Njuguna, J., Pielichowski, K., Silva, F., Zhu, H., 2013. Assessment of Nanoparticle Release from Polyamide 6- and Polypropylene-Silicon Composites and Cytotoxicity in Human Lung A549 Cells. *J. Inorg. Organomet. Polym.* 23, 861–870.

Jensen, K. A., Nørgaard, A. W., Koponen, I. K., Wolkoff, P., 2008. Characterization of Nanoparticles in the Air during Application of Commercial Nanofilm Coatings. 3rd International Conference on Surfaces, Coatings and Nanostructured Materials (NanoSMat), 21-24 October, 2008, Barcelona, Spain, Abstract Book, pp.20-21.

Joyce-Wöhrmann, R., Hentschel, T., Münstedt, H., 2000. Thermoplastic silver-filled polyurethanes for antimicrobial catheters. *Adv. Eng. Mater.* 2, 380–386.

Kaegi, R., Sinnet, B., Zuleeg, S., Hagendorfer, H., Mueller, E., Vonbank, R., Boller, M., Burkhardt, M., 2010. Release of silver nanoparticles from outdoor facades. *Environ. Pollut.* 158, 2900–2905.

Kaegi, R., Ulrich, A., Sinnet, B., Vonbank, R., Wichser, A., Zuleeg, S., Simmler, H., Brunner, S., Vonmont, H., Burkhardt, M., Boller, M., 2008. Synthetic TiO₂ nanoparticle emission from exterior facades into the aquatic environment. *Environ. Pollut.* 156, 233-239.

Li, J., Tong, L., Fang, Z., Gu, A., Xu, Z., 2006. Thermal degradation behavior of multi-walled carbon nanotubes/polyamide 6 composites. *Polym. Degrad. Stab.* 91, 2046-2052.

Liu, J., Katahara, J., Li, G., Coe-Sullivan, S., Hurt, R.H., 2012. Degradation products from consumer nanocomposites: A case study on quantum dot lighting. *Environ. Sci. Technol.* 6, 3220–3227.

Methner, M., Crawford, C., Geraci, C., 2012. Evaluation of the potential airborne release of carbon nanofibers during the preparation, grinding, and cutting of epoxy-based nanocomposite material. *J. Occup. Environ. Hyg.* 9, 308–318.

Mosurkal, R., Samuelson, L., Smith, K., Westmoreland, P., Parmar, V., Yan, F., Kumar, J., Watterson, A., 2008. Nanocomposites of TiO₂ and siloxane copolymers as environmentally safe flame-retardant materials. *J. Macromol. Sci., Part A: Pure Appl. Chem.* 45, 943–947.

Motzkus, C., Chivas-Joly, C., Guillaume, E., Ducourtieux, S., Saragoza, L., Lesenechal, D., Mace, T., 2011. Characterization of aerosol emitted by the combustion of nanocomposites. *J. Phys.: Conf. Ser.* 304:12020.

Nyden, M., Gilman, J., 1997. Molecular dynamics simulations of the thermal degradation of nano-confined polypropylene. *Comp. Theor. Polymer. Sci.* 7, 191–198.

Ogura, I., Kotake, M., Shigeta, M., Ueijima, M., Saito, K., Hashimoto, N., Kishimoto, A., 2013. Potential release of carbon nanotubes from their composites during grinding. *J. Phys.: Conf. Ser.* 429:012049.

- Olabarrieta, J., Zorita, S., Peña, I., Rioja, N., Monzón, O., Benburia, P., Scifo, L., 2012. Aging of photocatalytic coatings under a water flow: Long run performance and TiO₂ nanoparticle release. *Appl. Catal. B: Environ.* 182, 123–124.
- Raynor, P., Cebula, J., Spangenberg, J., Olson, B., Dasch, J., D’Arcy, J., 2012. Assessing potential nanoparticle release during nanocomposite shredding using direct-reading instruments. *J. Occup. Environ. Hyg.* 9, 1–13.
- Sachse, S., Gendre, L., Silva, F., Zhu, H., Leszczynska, A., Pielichowski, K., Ermini, V., Njuguna, J., 2013. On nanoparticles release from polymer nanocomposites for applications in lightweight automotive components. *J. Phys.: Conf. Ser.* 429:012046.
- Schlagenhauf, L., Chu, B., Buha, J., Nüesch, F., Wang, J., 2012. Release of carbon nanotubes from an epoxy-based nanocomposite during an Machining process. *Environ. Sci. Technol.* 46, 7366–7372.
- Van Landuyt, K. L., Hellack, B., Van Meerbeek, B., Peumans, M., Hoet, P., Wiemann, M., Kuhlbusch, T. A. J., Asbach, C., 2014. Nanoparticle release from dental composites. *Acta Biomaterialia.* 10, 365–374.
- Vilar, G., Fernández-Rosas, E., Puentes, V., Jamier, V., Aubouy, L., Vázquez-Campos, S., 2013. Monitoring migration and transformation of nanomaterials in polymeric composites during accelerated aging. *J. Phys.: Conf. Ser.* 429:012044.
- Voelker, D., Schlich, K., Hohndorf, L., Koch, W., Kuehnen, U., Polleichtner, C., Kussatz, C., Hund-Rinke, K., 2015. Approach on environmental risk assessment of nanosilver released from textiles. *Environ. Res.* 140, 661-672.
- Wohlleben, W., Meier, M. W., Vogel, S., Landsiedel, R., Cox, G., Hirth, S., Tomovic, Z., 2013. Elastic CNT-polyurethane nanocomposite: synthesis, performance and assessment of fragments released during use. *Nanoscale.* 5, 369–380.

Figures

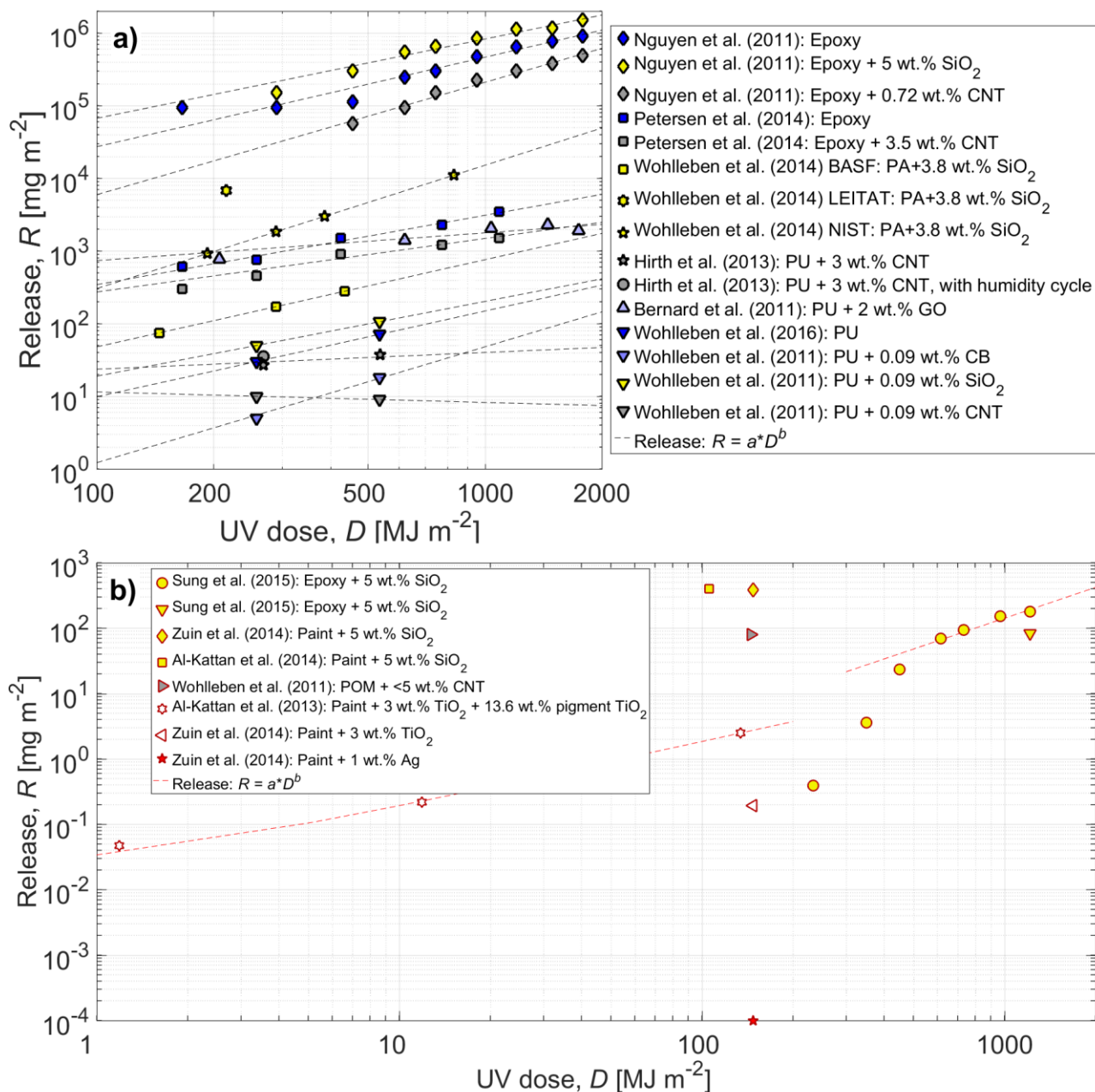


Figure 1. Release from artificial weathering as a function of UV dose: a) release of MAT+NM and b) release of NM without MAT. Table S7 shows aging protocols and sampling techniques for each study. Table S8 shows release function fitting parameters a and b .

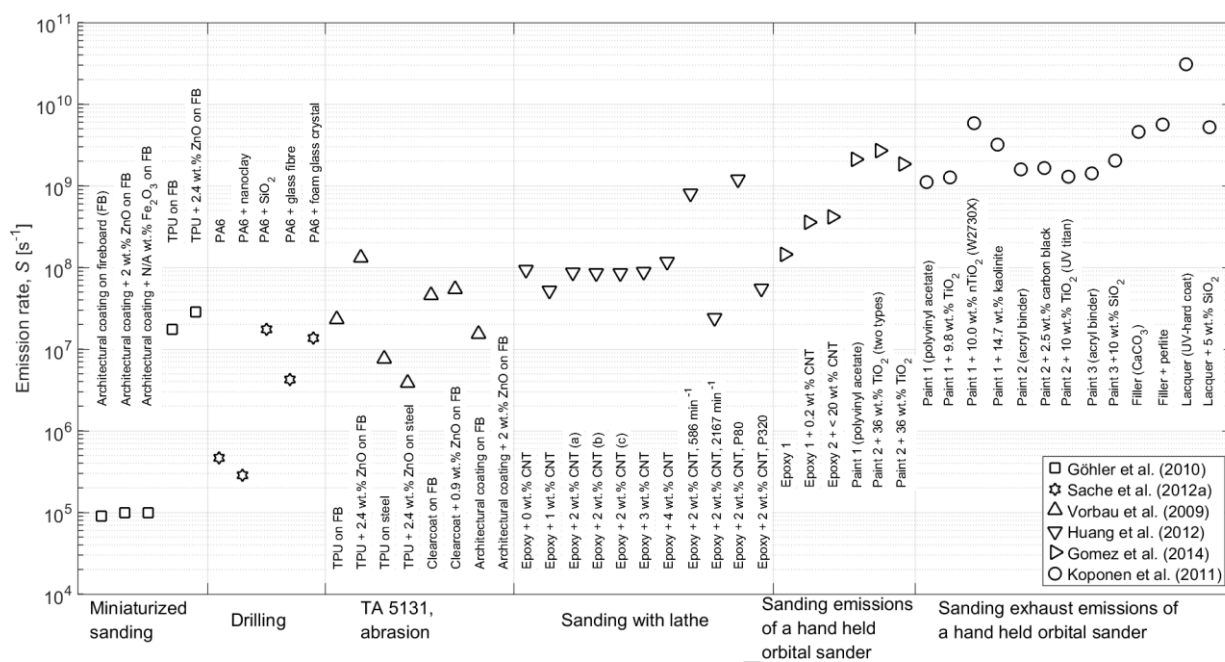


Figure 2. Particle number emission rates from mechanical treatment. The studies were ordered so that emission rate increases towards right hand side and not accordingly to the specific energy consumption or wear energy.

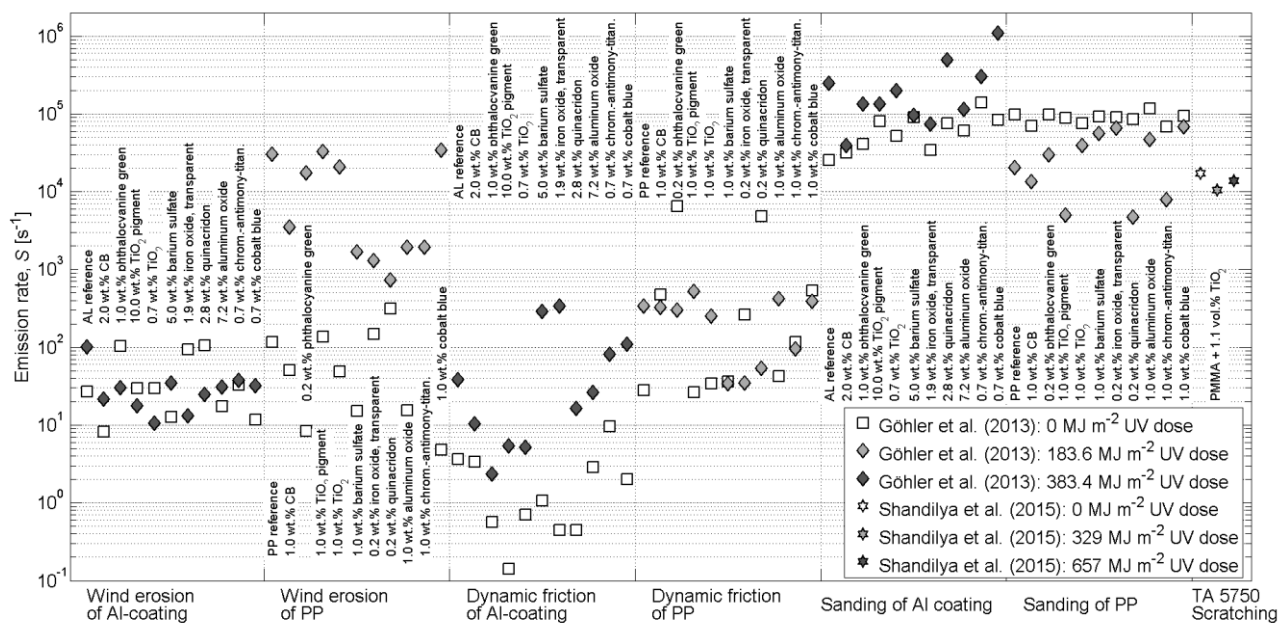


Figure 3. Particle emission rates for particles between 3 nm to 10 μm in diameter from mechanical treatment of weathered aluminum substrate with acrylate coating (Al-coating) and PP composites with pigment particles, and particle emission rates for particles between 4 nm to 3 μm in diameter scratching of PMMA composite.

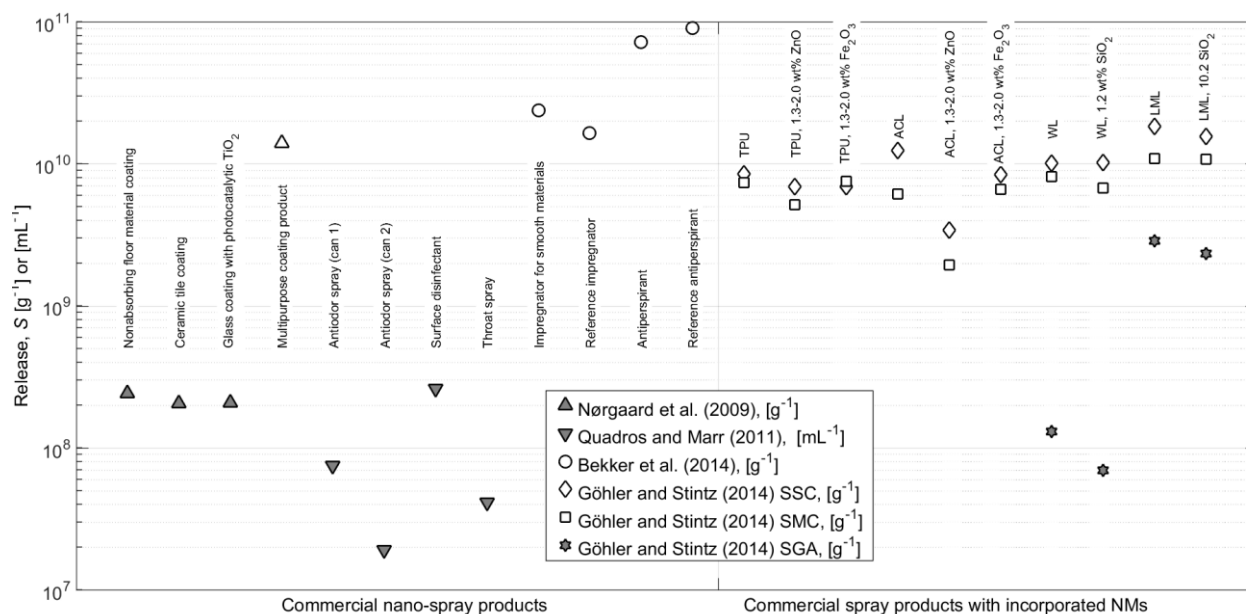


Figure 4. Particle emission rates from spraying process using pump sprays (shaded symbols), propellant sprays (open symbols), standard spray cans (SSC; open symbols) and SprayMax[®]-cans (SMC; open symbols), and manual gravity spray guns (SGA; shaded symbols). Göhler *et al.* (2014) incorporated NMs in TPU, Acrylate topcoat with TiO_2 pigment particles (ACL), water-based coating with TiO_2 pigment particles (WL) and organic solvent-based mixed coating (LML) which dry mass fractions are given.

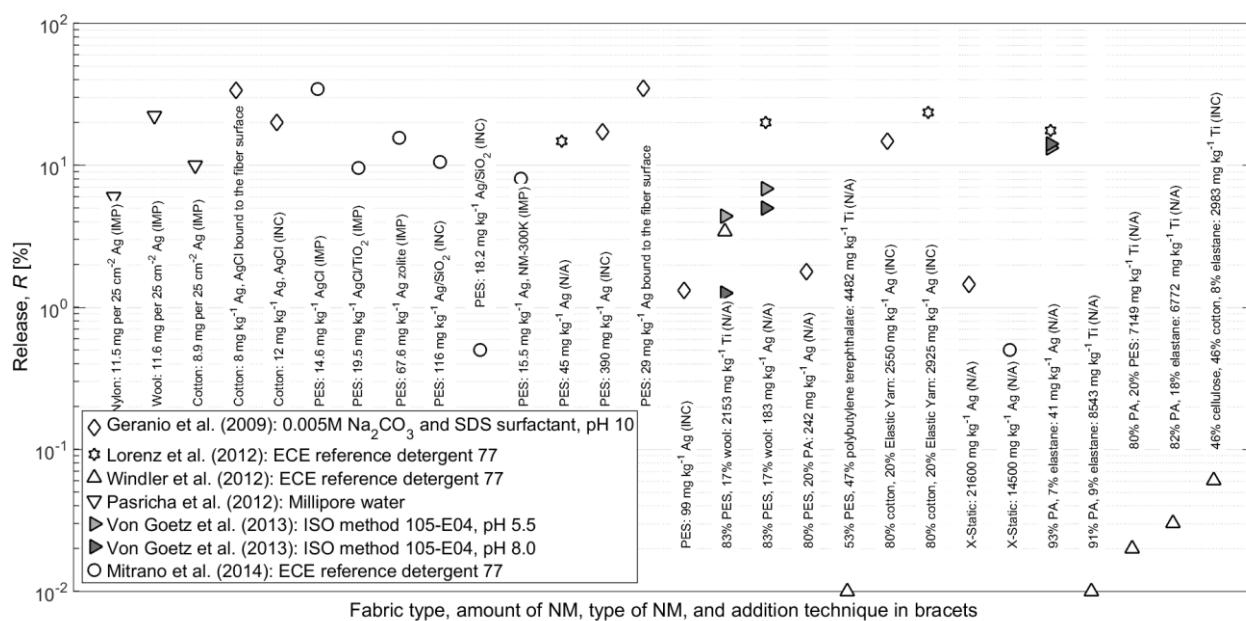


Figure 5. NM release in elemental fractions from textiles during first wash and rinse (open symbols) and leaching to different artificial sweats (shaded symbol). NM applying techniques are shown as incorporation (INC) or impregnation (IMP). Detection limit values were 1.25 and $1.5 \text{ mg}\cdot\text{kg}^{-1}$ for Lorenz *et al.* (2012) and Von Goetz *et al.* (2013), respectively.

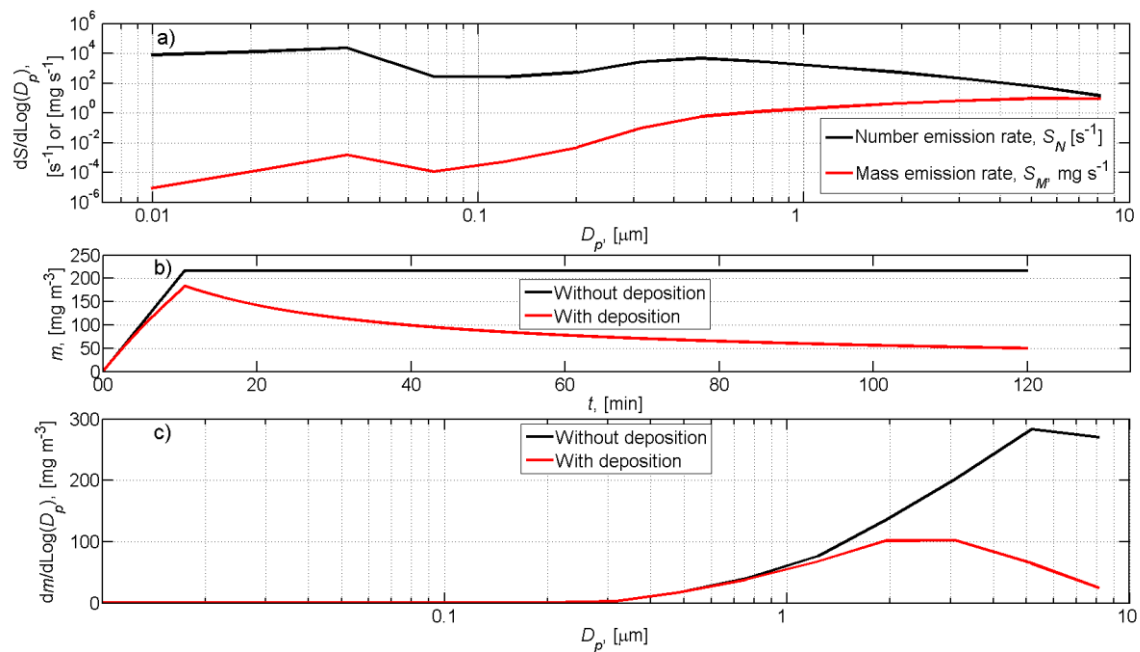


Figure 6. Emission rate modelings showing a) size resolved particle number emission rates and mass emission rates, b) mass concentrations released during 21 minutes and 15 second sanding, and c) averages of mass size distributions measured



Graphical abstract

ACCEPTED MANUSCRIPT

Highlights

- Quantitative releases were derived from existing emission studies.
- Properties of released fragments were summarized.
- Establishes a quantitative emission library for articles containing nanomaterials.
- Examples how to use the data for exposure assessment based on mass flows.
- Recommendations for quantitative release measurements.

ACCEPTED MANUSCRIPT